

## MASTER

### Design of an automated guided vehicle supporting an order picking robot for the warehouse of the future

van Loon, T.J.

*Award date:*  
2019

[Link to publication](#)

#### **Disclaimer**

This document contains a student thesis (bachelor's or master's), as authored by a student at Eindhoven University of Technology. Student theses are made available in the TU/e repository upon obtaining the required degree. The grade received is not published on the document as presented in the repository. The required complexity or quality of research of student theses may vary by program, and the required minimum study period may vary in duration.

#### **General rights**

Copyright and moral rights for the publications made accessible in the public portal are retained by the authors and/or other copyright owners and it is a condition of accessing publications that users recognise and abide by the legal requirements associated with these rights.

- Users may download and print one copy of any publication from the public portal for the purpose of private study or research.
- You may not further distribute the material or use it for any profit-making activity or commercial gain

---

# Design of an automated guided vehicle supporting an order picking robot for the warehouse of the future

---

DC 2019.068

T.J. van Loon BSc., 0861750

## Committee:

prof. dr. H. Nijmeijer (chairman)  
dr. ir. P.C.J.N. Rosielle (thesis supervisor)  
dr. ir. R.H.J. Peerlings  
ir. M.M.G. van Lith (advisor)



EINDHOVEN UNIVERSITY OF TECHNOLOGY  
DEPARTMENT OF MECHANICAL ENGINEERING  
DYNAMICS AND CONTROL GROUP

21 JUNE 2019

## Summary

Web shops offer customers the luxury of shopping from the comfort of their homes. The orders sent by customers have to be fulfilled by order pickers. Order pickers compile orders from individual items which are stockpiled in a warehouse. Companies want to automate the order picking process in order to make their entire supply chain more efficient.

Warehouse automation is often based on conveyer belts that transport items to picking stations, where order pickers compile the individual orders. Such systems reduce the time that would otherwise be spent by an order picker walking through the warehouse with a trolley. However, such order picking systems are a large investment, and are not scalable.

Smart Robotics, EPhi and Nobleo Technology want to create an order picking robot. This robot should be able to perform all tasks a human order picker performs as well: Navigating autonomously through a warehouse, picking items from racks, and leaving the compiled order at a drop-off point. A prototype has been built, which consists of an AGV supporting a 6 degree-of-freedom robotic arm, and a conveyer which holds a container.

To improve the order picking robot, front- and rear wheels suspensions are designed. With the new suspension design the order picking robot can corner faster, and is more robust to floor surface irregularities. The prototype AGV has two individually driven rear wheels, and two casters at the front. The newly designed AGV has its rear wheels driven, and its front wheels steered using an Ackerman linkage. This decouples longitudinal and lateral motion, which is beneficial for maintaining velocity while cornering. By replacing the casters with steered wheels more lateral force can be exerted on the floor by the AGV. This means that the AGV can corner faster.

The front suspension is based on the McPherson strut suspension design. The wheels are connected to uprights. On the top, the upright is attached to a damper. The centerline of the damper points to a ball joint between the upright and a leaf spring. The leaf spring is mounted to the bottom of the frame. The piston of the damper can freely rotate in its housing. Therefore the wheel can be steered around the centerline of the damper. The steering is actuated by using a Pitman arm. The pitman arm consists of partial gears which are driven using a pinion attached to an electric motor inside of the frame.

The rear wheel suspension is built around an axle containing a steel spur gear differential. The spur gear differential is directly connected to the wheels by tubular shafts that are also contained within the hollow axle. The axle is connected to an A-frame from the top, and to two longitudinally placed struts close to the wheels on the bottom. The weight of the frame is carried by two shock absorbers.

## Contents

<b>1</b>	<b>Introduction</b>	<b>1</b>
1.1	Background . . . . .	1
1.2	Automating the order picking process . . . . .	2
1.3	Objective . . . . .	2
1.4	Current solution . . . . .	3
1.5	Project aim . . . . .	4
<b>2</b>	<b>Specifications</b>	<b>5</b>
2.1	Low cost design . . . . .	5
2.2	Compact design . . . . .	5
2.3	Able to support the weight of the order picking robot . . . . .	5
2.4	Robustness to rough floor surfaces . . . . .	6
2.5	Safe to use around human personnel . . . . .	6
2.6	Capable of withstanding the tire forces during travel . . . . .	7
2.6.1	Wheel modelling . . . . .	7
2.6.2	Load on wheels during acceleration . . . . .	8
2.6.3	Load on wheels during deceleration . . . . .	8
2.6.4	Maximum velocity during straight line driving . . . . .	9
2.6.5	Load on wheels during cornering . . . . .	9
2.7	Able to remain operational for a specified lifetime . . . . .	12
2.8	Summary . . . . .	14
<b>3</b>	<b>Overall design</b>	<b>15</b>
3.1	Wheel force comparison . . . . .	15
3.2	Ackermann steering . . . . .	16
3.3	Tire choice . . . . .	19
3.4	Wheel construction . . . . .	20
<b>4</b>	<b>Front wheel suspension</b>	<b>21</b>
4.1	Construction of the upright . . . . .	22
4.2	Pitman arm . . . . .	23
4.3	Leaf spring . . . . .	24
<b>5</b>	<b>Rear wheel suspension</b>	<b>26</b>
5.1	Rear wheel drive and suspension concepts . . . . .	26
5.1.1	Electronic differential . . . . .	26
5.1.2	Mechanical differential using Nylon gears . . . . .	28
5.1.3	Mechanical differential using Steel gears . . . . .	32
5.1.4	Concept choice . . . . .	34
5.2	Differential construction . . . . .	34
5.3	Axle assembly . . . . .	35
5.4	Construction of the A-frame and the struts . . . . .	37
<b>6</b>	<b>Conclusion</b>	<b>38</b>
<b>7</b>	<b>Recommendations</b>	<b>38</b>

# 1 Introduction

The current rise of web shops puts an increasing strain on logistics, with many web shops even promising to deliver goods to the customer in less than 24 hours. These demands can only be met because of growth in the transportation sector and various smart warehousing solutions. In the case of web shops, the focus is on making *order picking* more efficient. Order picking describes the act of gathering items from a warehouse, and bringing them to a drop-off point. This is done by dedicated personnel called *order pickers*.

## 1.1 Background

In order to conceptualize the layout of a typical warehouse DSV was visited. DSV is a logistic company. A photo of the inside of the warehouse is shown in Figure 1.1. Their warehouse features many narrow corridors. These are formed by racks filled with cardboard boxes, which are accessible from the sides. The items contained in these boxes are packed in small plastic bags, with a maximum weight of 2 kilograms. Packing items in plastic bags is common practice in warehouses. The order pickers use slim trolleys on which they carry multiple container. In each of these containers they need to collect a certain order.



**Figure 1.1:** A typical warehouse

The corridors are  $1500 [mm]$  wide. The trolleys are  $600 [mm]$  wide. This means that an order picker has the possibility to overtake another order picker who has stopped to fill some of their containers, while still keeping  $100 [mm]$  of clearance on each side of their trolley. An order picker has to systematically walk through a warehouse to collect each order. They gather the contents of an order in a container. To reduce human errors during picking, order pickers are aided by *warehouse management software*, which tells them what item to pick next. Warehouse management software helps web shops to keep track of their inventory, while it allows order pickers to keep track of the items they have to collect. Multiple orders can be combined in a batch. By fulfilling batches of orders instead of separate orders the order picker spends less time walking through the warehouse. This reduces picking times.

## 1.2 Automating the order picking process

An order picker can easily grab items out of a cardboard box. However, a robot often struggles with such a task because the location of the item in the cardboard box is not determined exactly. Next to this, various different items need to be handled. This makes order picking inherently difficult for robots. This is the reason why robotic order pickers still are less efficient than a human order picker. However, the power of automating the order picking is that the process can be made more predictable, in terms of how long it takes to fulfill an order. This allows companies to optimize their entire supply chain.

Currently available warehouse automation aims to bring the cardboard boxes to *picking stations* using conveyer belts. At these picking stations, order pickers compile orders from the incoming cardboard boxes. Such order picking systems are a large investment, typically in the range of 10 million euros. It also takes a long time to install the system in a warehouse, as the warehouse needs to stay in operation to avoid loss in revenue for the company. When the system is installed, it is not scalable. This means that when the capacity of the warehouse should increase, or when the range of products stored in the warehouse is altered, the order picking automation needs to be rebuilt. Next to this, the throughput of a warehouse can periodically change throughout the year, while the order picking automation is designed for peaks in the throughput.

## 1.3 Objective

Some companies envision a warehouse robot that can execute most tasks a human order picker can perform, including:

- Autonomously navigating through a warehouse
- Picking items from a cardboard box in a rack
- Delivering an order at a drop-off point

Buying one robot allows a company to partially automate their warehouse. The robot needs to be designed to allow for easy commissioning by any warehouse. Robots could be used during peak moments in a warehouse, while they can be stored or used somewhere else when the demand on the supply chain is not as large. The return upon investment of such a robot would then be faster than buying an entire automated warehouse. The solution is scalable, as multiple parts of the warehouse can be automated by buying more robots. Having robots work alongside order pickers could result in conflicts, if the order pickers feel threatened by the robots. It should therefore be considered to divide the warehouse in robot-only and human-only parts.

The robot should be applicable in different warehouses. While new warehouses often have smooth concrete floors, the floors in older warehouses might have a lot of irregularities. An AGV carrying such a warehouse robot therefore needs to be robust to irregularities in floors. The order picking robot should be designed to operate in a warehouse without additional infrastructure. The layout of the warehouse could thus be maintained, reducing the overall cost of automating (parts of) a warehouse.

## 1.4 Current solution

Three companies, SmartRobotics, Nobleo Technology and EPhi, want to create an *order picking robot* in a joint effort. The current prototype of the order picking robot consists of an automated guided vehicle (AGV) supporting a 6 degrees-of-freedom robotic arm and an on-board conveyer which can hold a container. This can be seen in Figure 1.2.

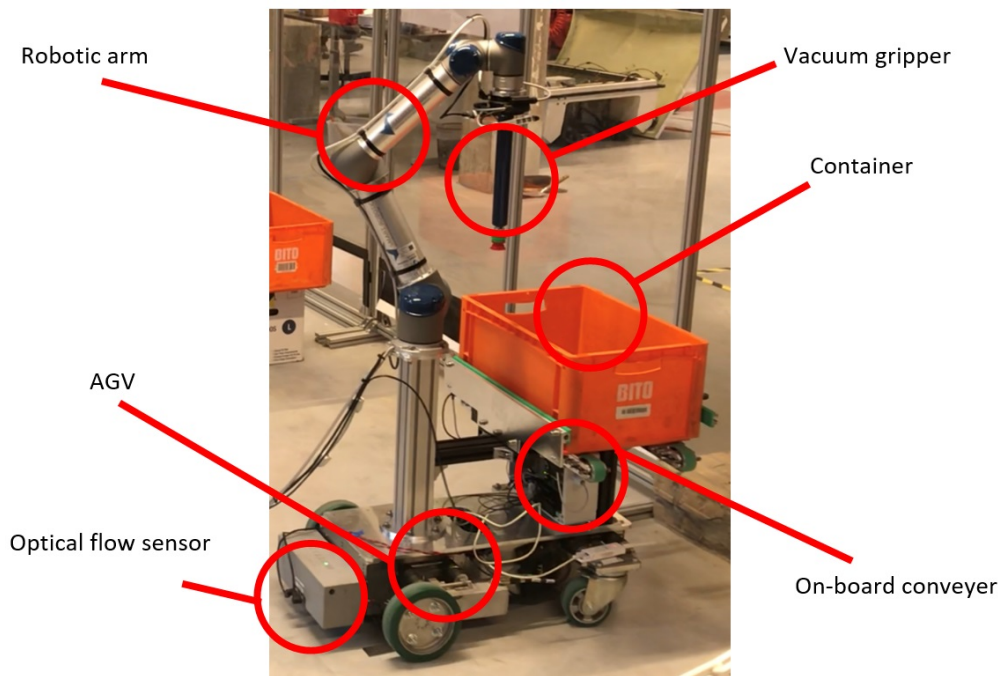


**Figure 1.2:** Prototype of the order picking robot

This prototype is built out of spare parts, and is used to demonstrate the functionality of the order picking robot to potential customers. To realize the autonomous navigation a laser range finder system is used in combination with an optical flow sensor. The laser range finder can scan the direct surroundings of the order picking robot, ensuring that it does not collide with its environment. The optical flow sensor features two cameras pointed at the floor, which keep track of the AGV's orientation. This particular sensor, an Accerion Jupiter-40, can also keep track of the exact location of the order picking robot. It captures images of the floor surface, and therefore remembers which patches of the floor it has already seen. The overall dimensions of the AGV can be found in Figure 1.3.

The AGV used in the current prototype of the order picking robot is produced by Nobleo Technology. The AGV's front wheels are casters. By individually driving the rear wheels using electric motors, the AGV can be driven and steered. Because casters are used at the front of the AGV, the wheelbase can vary anywhere between 460 [mm] and 520 [mm]. The front track width can vary between 360 [mm] and 600 [mm]. It is therefore hard to estimate how the load of the order picking robot is distributed over the wheels of the AGV at any given point in time. This results in an unpredictable performance of the AGV during straight-line driving as well as during cornering. Figure 1.4 shows that the suspension of the AGV is not able to support the full weight of the order picking robot without reaching the end stops. This leaves no room for any wheel travel during bumps.

Next to this, it also reduces the clearance between the bottom of the AGV and the floor.

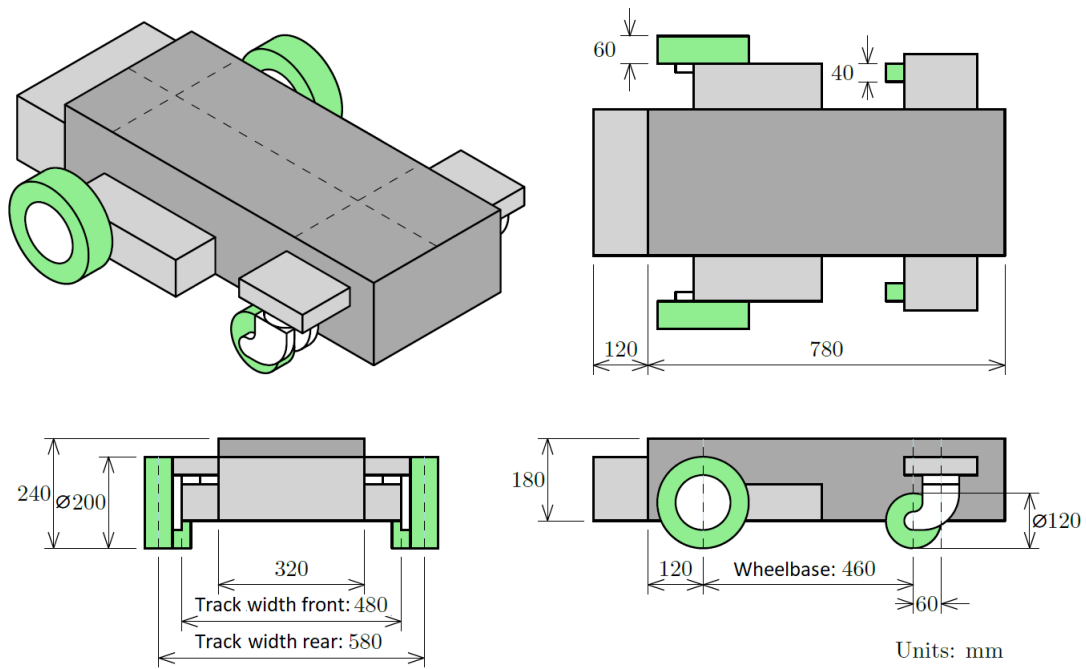


**Figure 1.3:** Overall dimensions of the current AGV



**Figure 1.4:** Sagging of the AGV's suspension

## 1.5 Project aim

The aim of the project is to design a new AGV for the prototype of the order picking robot. The new AGV should be able to carry the load of the order picking robot, corner faster than the current AGV, and be more robust to floor surface irregularities.



## 2 Specifications

The development of the order picking robot is a 'technology push' type of project. This means that the specifications for the order picking robot are not determined by a customer. The specifications for the AGV are therefore discussed in the following Sections.

### 2.1 Low cost design

The goal of the project is to create low-cost automation for warehouses. When the order picking robot turns out to be a feasible solution for warehouse automation, its design should allow mass production. Therefore the prototype for the new AGV should be built out of low-cost components that are readily available. The assembly of the AGV should be straightforward. This also allows for easy maintenance of the AGV, which reduces the costs for operating the order picking robot.

### 2.2 Compact design

The AGV should have a small footprint. This is necessary to allow an order picking robot to overtake another order picking robot that stopped to pick items from a tote in a rack. The trolleys used by order pickers in the warehouse are 600 [mm] in width. The current prototype of the order picking robot does not yet contain all the necessary equipment it needs to perform in a warehouse. The new design should therefore offer more space for the additional components. For this reason a maximum length of 900 [mm] is chosen. To maximize the wheelbase, a wheel diameter of 150 [mm] and wheel width of 50 [mm] is chosen. The wheelbase and track width of the AGV are therefore 750 [mm] and 550 [mm] respectively.

### 2.3 Able to support the weight of the order picking robot

The AGV should support a robotic arm, the controller for this robotic arm, a conveyer, a battery pack, and a payload. The approximate weight of these items are presented below.

Robotic arm:	30 [kg]
Robotic arm controller:	20 [kg]
Conveyer:	20 [kg]
Battery pack:	15 [kg]
Payload:	10 [kg]
AGV:	55 [kg]
Total:	150 [kg]

An estimation for the location of the center of mass of the order picking robot needs to be made in order to estimate the load supported by each wheel. It is also used in modelling the forces acting on the AGV during acceleration, deceleration and cornering. Figure 2.1 is used to approximate the center of mass of the order picking robot. It is based on the current layout of the order picking robot. The location of the additional components is estimated. Without a payload the center of mass lies approximately 400 [mm] from the rear of the AGV, and 300 [mm] above the floor. Including the payload, the center of mass lies 350 [mm] above the floor.

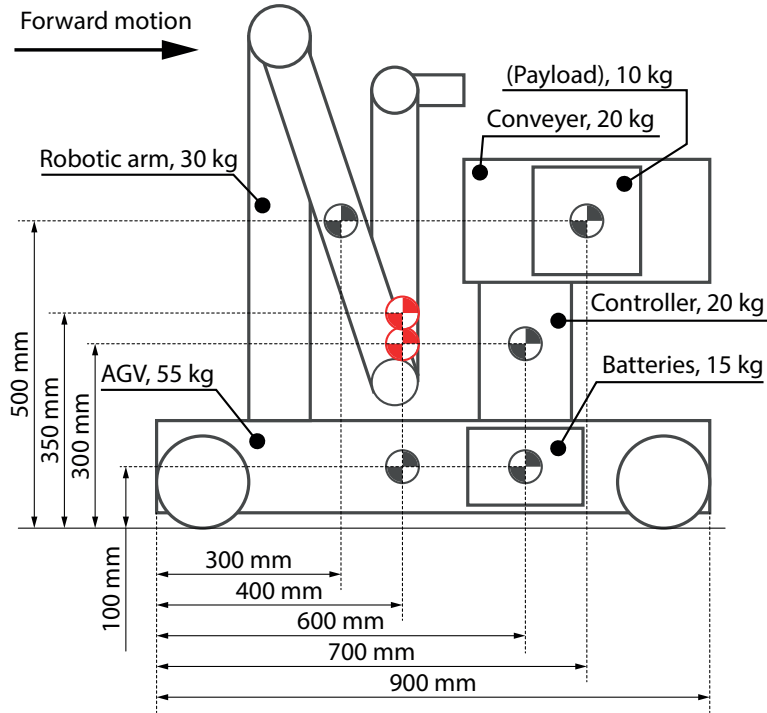


**Figure 2.1:** Schematic overview of the order picking robot. The center of mass for a loaded and unloaded order picking robot are indicated in red.

While unloaded, the axle loads on the front and the rear of the AGV are equal to  $605 [N]$  and  $795 [N]$  respectively. While loaded, the axle loads on the front and the rear of the AGV are equal to  $850 [N]$  and  $650 [N]$  respectively.

## 2.4 Robustness to rough floor surfaces

Because the order picking robot needs to be a fit-for-all solution, the AGV needs to be able to drive over different kinds of floor surfaces. The AGV should be able to handle different floor surfaces without excessive wear of any components. Therefore the unsprung mass of the AGV needs to be as low as possible. The clearance between the bottom of the AGV and the floor should be at least  $30 [mm]$ . This is to ensure that the bottom of the AGV does not collide with the floor.

## 2.5 Safe to use around human personnel

As the order picking robot will be used around human personnel, it should be aware of its surroundings. When an order picker crosses its path, it should be able to stop in time. It seems reasonable to assume that the AGV should be able to bring the order picking robot to a full stop within  $0.5 [m]$ . The AGV should also be constructed in such a way that tipping over of the order picking robot is avoided. When an order picking robot tips over, it could injure order pickers or damage other warehouse equipment.

## 2.6 Capable of withstanding the tire forces during travel

During acceleration, deceleration and cornering, load is transferred over the wheels of the AGV. The load distribution is important for the design of the wheel suspension. To calculate the load transfer during the beforementioned maneuvers, first a simple wheel model is presented. This is used to calculate the forces exerted by the wheels on the floor surface. The maximum acceleration and deceleration are calculated, and the load transfer during these maneuvers is calculated. The maximum velocity of the AGV is calculated using the specified stopping distance and the minimum deceleration. Next, the maximum cornering velocity is calculated, as well as the load transfer during cornering.

### 2.6.1 Wheel modelling

Tires can exert forces on a floor surface. These forces are generated in the contact patch between the tire and the floor. Lateral forces can be generated parallel to the axle through the wheel hub, and longitudinal forces tangent to the circumference of the wheel. This is visualized in Figure 2.2, where the force  $\vec{F}_{tire}$  represents the maximum resultant force that can be generated by the wheel.

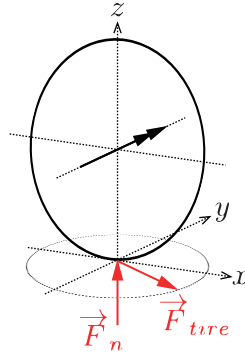


**Figure 2.2:** Tire friction circle

The magnitude of the force  $\vec{F}_{tire}$  can be described as a factor of the magnitude of the normal load  $\vec{F}_n$  acting on the wheel, which is referred to as the tire friction coefficient  $\mu$ :

$$\vec{F}_{tire} = \mu \vec{F}_n$$

This wheel model is referred to as the tire friction circle. This force can be exceeded when the AGV is forced to accelerate faster than its wheels allow it to. The wheels will then start to slip, which results in loss in traction. For pneumatic tires on asphalt, the tire friction coefficient is generally 0.7 [–] for dry roads and 0.4 [–] for wet roads. This range of values will be used to investigate the behavior of the AGV. The tire friction circle does not account for the following:

- In general, tires can exert more force longitudinally than laterally. The sum total of the forces a tire can exert on the floor surface is therefore dependent on the direction in which the force needs to be applied.
- The tire coefficient itself also depends on the magnitude of the normal load. In situations where load is transferred over the wheels, for example during cornering or acceleration, the tire friction coefficient changes [1]. In most cases this results in a loss of traction.

### 2.6.2 Load on wheels during acceleration

The maximum acceleration is restricted by the size of the wheelbase in combination with height of the center of mass above the floor. The maximum acceleration is also restricted by the maximum traction that the wheels can deliver. Using Figure 2.3, weight distribution over the front and the rear wheels can be determined by applying moment balance. To determine the maximum allowable acceleration, the payload weight has been included, and the corresponding center of mass location has been used.

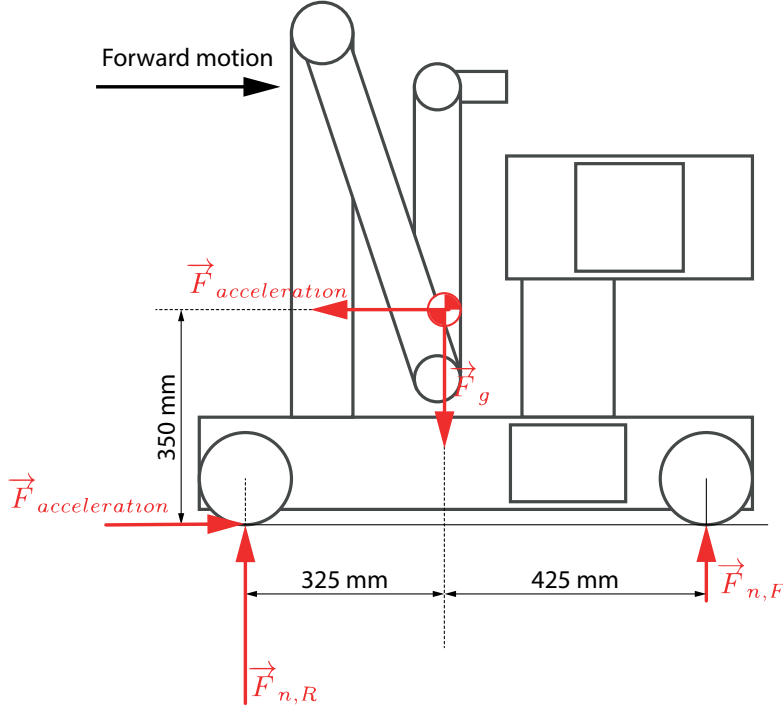


**Figure 2.3:** AGV during acceleration

Based on wheel traction, the highest acceleration is limited to  $4 \left[ \frac{m}{s^2} \right]$ . This would be the maximum acceleration if all the wheels contributed to acceleration the AGV. During an acceleration of  $4 \left[ \frac{m}{s^2} \right]$  the axle loads on the front and rear of the AGV are equal to  $370 [N]$  and  $1130 [N]$  respectively. All of the AGV's wheels therefore remain in contact with the floor during acceleration. Using the wheel radius, the torque on the driving axle can be calculated. Achieving an acceleration of  $4 \left[ \frac{m}{s^2} \right]$  with a rear wheel drive results in  $23 [Nm]$  of torque on an individual rear wheel.

### 2.6.3 Load on wheels during deceleration

The maximum deceleration based on the wheel traction is  $7 \left[ \frac{m}{s^2} \right]$ . During this deceleration the axle loads on the front and rear of the AGV are  $1140 [N]$  and  $360 [N]$  respectively. Therefore all the tires of the AGV remain in contact with the floor.

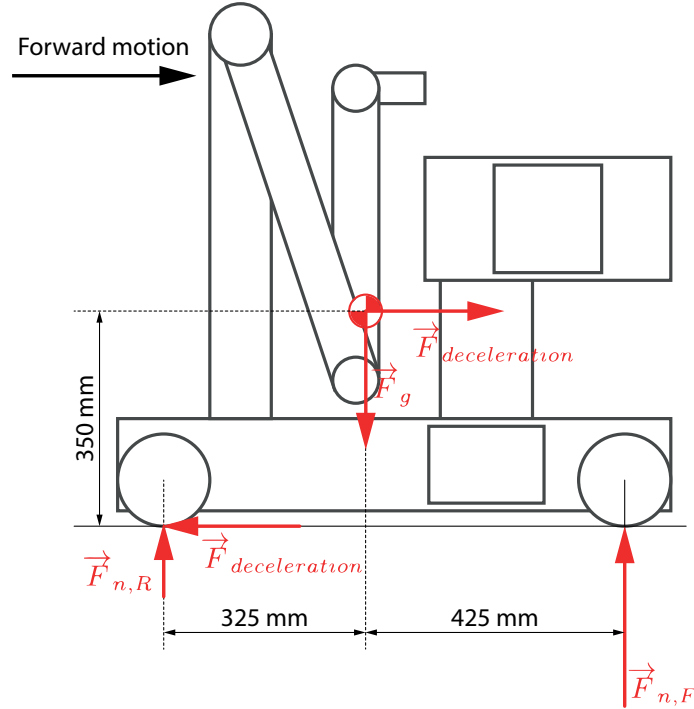


**Figure 2.4:** AGV during deceleration

#### 2.6.4 Maximum velocity during straight line driving

The maximum velocity can be determined using the maximum stopping distance  $x = 0.5 [m]$  and the minimum deceleration  $d_{min} = 4 [\frac{m}{s^2}]$ . Assuming an instantaneous and constant deceleration following the moment of detecting an order picker in the path of the order picking robot, the stopping time can now be calculated:

$$x = \frac{1}{2}d_{min}t^2$$

Where  $t$  is the time it takes the AGV to come to a full stop. This time is equal to  $t = 0.5 [s]$ . The maximum velocity before the onset of the deceleration would therefore be:

$$v = d_{min}t$$

Where  $v = 2 [\frac{m}{s}]$  is the maximum velocity during straight line driving. When a higher tire friction coefficient can be achieved the maximum velocity can of course be higher. However, floor surface irregularities or fluid spills can reduce the amount of traction the AGV has. Therefore  $v = 2 [\frac{m}{s}]$  is kept as the maximum velocity.

#### 2.6.5 Load on wheels during cornering

The maximum velocity during steady-state cornering depends on the height of the center of mass, the track width and the tire friction coefficients. As the AGV needs to be able to come to a full stop at all times, the cornering velocity also depends on the maximum stopping distance  $x = 0.5 [m]$ . The longitudinal force that can be used to decelerate the AGV is limited by the lateral force needed for cornering. The lateral acceleration  $a_{lateral}$  needed for cornering can be determined by:

$$a_{lateral} = \frac{v_{corner}^2}{r_{corner}}$$

Where  $v_{corner}$  is the cornering velocity and  $r_{corner} = 1.1 [m]$  is the cornering radius. The maximum deceleration  $d_{min}$  can now be calculated as follows:

$$d_{min} = \sqrt{(\mu g)^2 - a_{lateral}^2}$$

Where  $\mu$  is the tire friction coefficient and  $g$  the gravitational acceleration. The velocity  $v_{safestop}$  at which the AGV can come to a halt within  $x = 0.5 [m]$  can now be calculated:

$$v_{safestop} = d_{min} \sqrt{\frac{2x}{d_{min}}}$$

The result of this analysis can be found in Figure 2.5, where  $\mu = 0.4 [-]$  has been used.

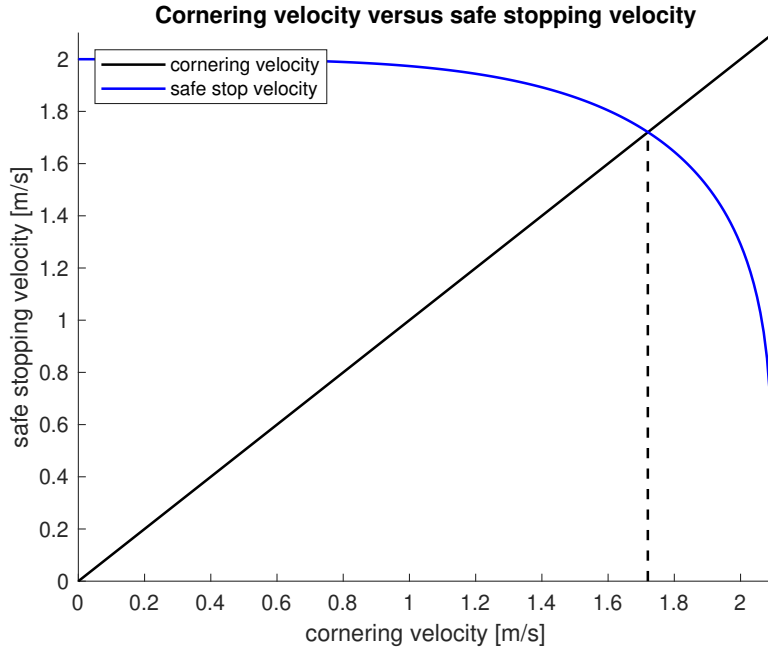


**Figure 2.5:** Plot of the cornering velocity versus the velocity at which the AGV can safely come to a full stop.

Around  $v_{corner} = 1.7 [\frac{m}{s}]$  it can be observed that the cornering velocity is too high to come to a full stop within  $x = 0.5 [m]$ . Keeping a margin to compensate for the simplicity of the wheel modelling, the maximum cornering velocity will be set to  $v_{corner} = 1.5 [\frac{m}{s}]$ .

To get a feeling for the velocity at which the AGV starts slipping or starts tipping over, the model in Figure 2.6 is utilized. The force  $\vec{F}_{corner}$  is equal to:

$$\vec{F}_{corner} = m_{OPR} \frac{v_{corner}^2}{r_{corner}}$$

Where  $m_{OPR}$  represents the mass of the order picking robot. When the normal force on the inside wheel,  $\vec{F}_{n,L}$ , is taken equal to zero, the cornering speed that leads to tipping of

the order picking robot can be found. Note that the assumption is made that the center of mass of the AGV would roll around the contact patch between the floor surface and the outer tire. This is not how the AGV would behave in real life, where the center of mass would roll around the roll axis defined by the roll centers of both the front- and the rear wheel suspension.

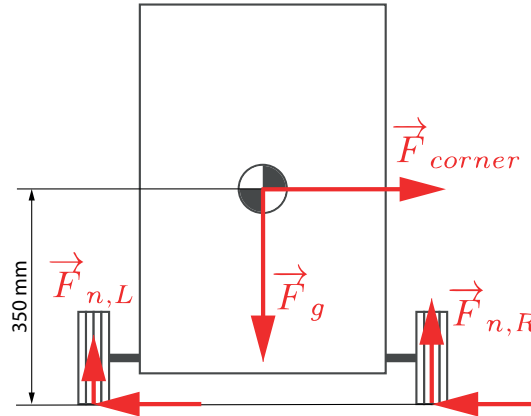


**Figure 2.6:** Tipping model. The center of mass of an order picking robot carrying a payload is used.

The maximum lateral traction that can be achieved is equal to  $m_{OPR}\mu g$ . Using this criterion the maximum steady-state cornering velocity can be found at which the AGV starts slipping. Using the specified track width of 550 [mm], Figure 2.7 is obtained for varying center of mass locations.

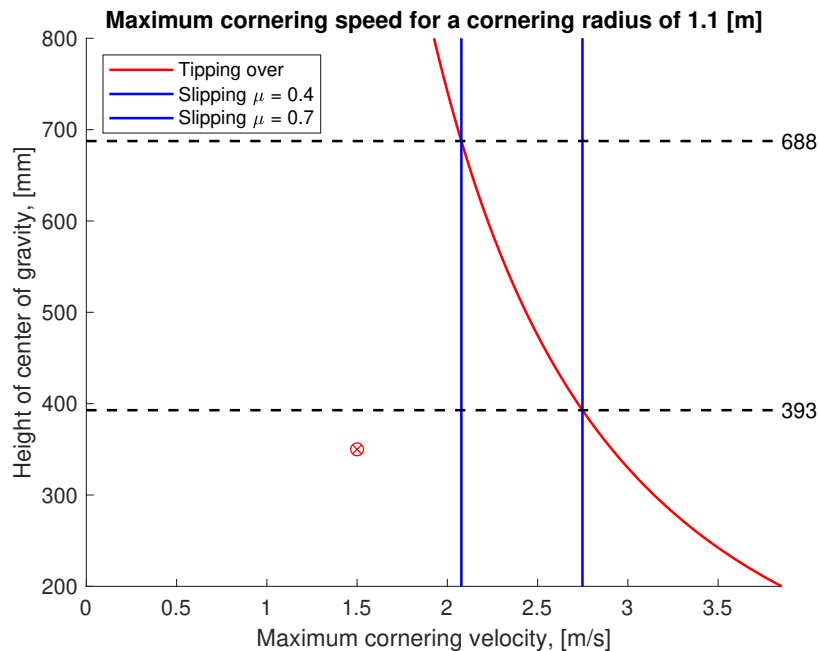


**Figure 2.7:**  $v_{corner}$  versus center of mass height using the criteria for slipping and tipping over. The specified  $v_{corner} = 1.5 \left[ \frac{m}{s} \right]$  is plotted versus the center of mass of the loaded order picking robot.

When the center of mass is more than 688 [mm] above the floor, the AGV tips over if

the cornering velocity is too high. For a center of mass that is between 393 [mm] and 688 [mm] above the floor it depends on the tire friction coefficient whether or not the AGV tips over. If the center of mass of the AGV is below 393 [mm] the AGV will start slipping at high cornering velocities, instead of tipping over. The latter is a more desirable situation, as tipping could cause damage to the robotic arm of the order picking robot. For a center of mass at a height of 350 [mm] a cornering velocity of  $v_{corner} = 2.1 \left[ \frac{m}{s} \right]$  can be reached before the AGV starts slipping. As can be seen, a maximum cornering velocity of  $v_{corner} = 1.5 \left[ \frac{m}{s} \right]$  will therefore ensure that the AGV can still come to a full stop within the required distance, whilst not slipping or tipping over during cornering. Using the model in Figure 2.6 the load on the wheels can also be calculated for a given cornering velocity. For the chosen cornering velocity of  $v_{corner} = 1.5 \left[ \frac{m}{s} \right]$  the load on the inner- and outer wheels is 555 [N] and 945 [N] respectively.

## 2.7 Able to remain operational for a specified lifetime

It is desired to have an estimation for the total amount of wheel rotations, and the difference in wheel rotations in corners, in order to design a drive train. Figure 2.8 shows a partial floorplan of a typical warehouse.

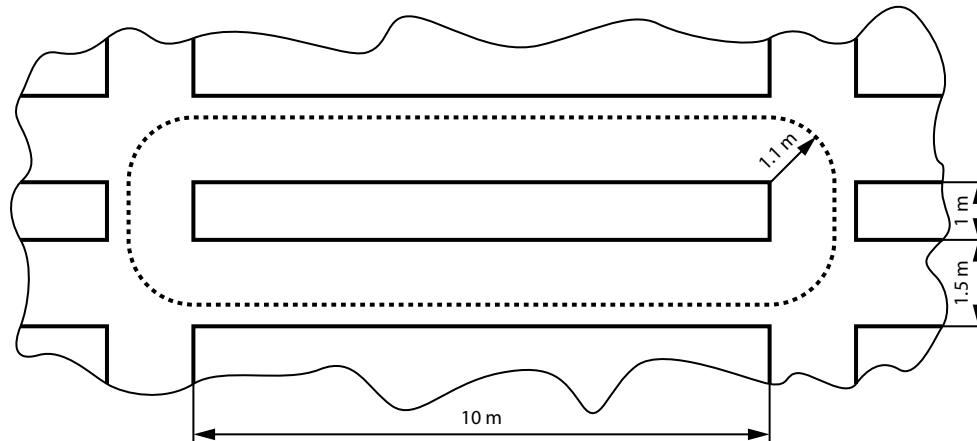


**Figure 2.8:** Partial floorplan of a typical warehouse. The dotted line indicates the trajectory of a trolley used by an order picker.

This trajectory runs around a single rack, forming a lap. Such a lap is representative of the trajectory the order picking robot would need to follow. After all, taking a corner either to the left or to the right results in the same distance travelled. Therefore this lap will be used to determine the total distance travelled during the lifetime of the order picking robot. To model the total distance travelled by the order picking robot during its lifetime it is assumed it has to stop four times per lap to pick an item. Experiments with the current prototype showed that picking an item takes 20 seconds. The order picking robot travels with a velocity of  $2 \left[ \frac{m}{s} \right]$  in between picks, and with a velocity of  $1.5 \left[ \frac{m}{s} \right]$  in corners. When the order picking robot has to change velocity, a constant rate of  $4 \left[ \frac{m}{s^2} \right]$  and  $7 \left[ \frac{m}{s^2} \right]$  for acceleration and deceleration respectively is used. With these assumptions, the velocity profile in Figure 2.9 is obtained.



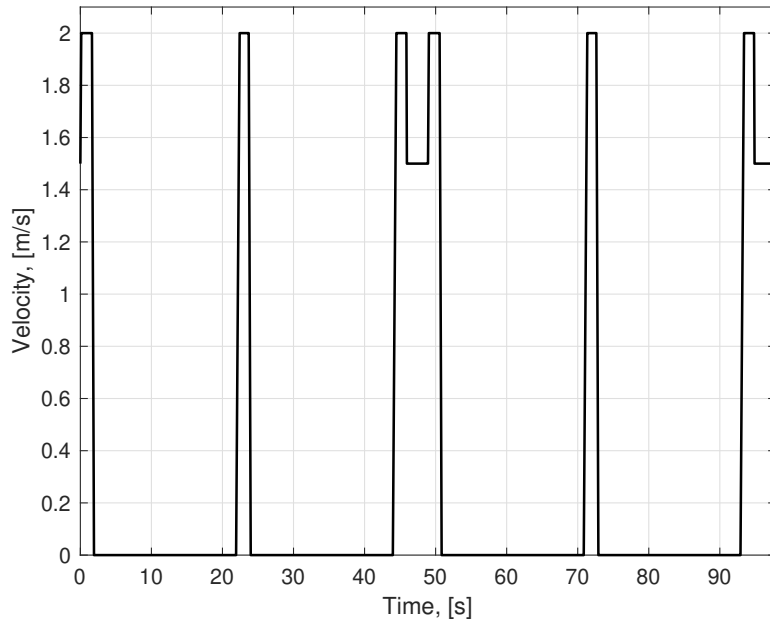


**Figure 2.9:** Velocity profile of the order picking robot through the warehouse 'lap'

The total distance travelled in one lap is  $29 [m]$ . The time it takes the order picking robot to complete one lap is approximately  $100 [s]$ . As the order picking robot runs on batteries, it needs to recharge when the battery is depleted. It is estimated that the order picking robot can stay operational for 10 hours a day. This means the order picking robot travels approximately finishes 360 laps per day, which is roughly equal to  $11 [km]$ . The average velocity of the order picking robot is therefore  $1.1 [\frac{km}{h}]$ . The lifetime of the order picking should be at least 5 years. It therefore travels  $20000 [km]$  in total over its lifetime. The lap under consideration only features corners in one direction. When the order picking travels through the warehouse, it will make corners in both directions. Therefore it is assumed that all tires are exposed to an equal amount of rotations. Using the diameter of the tires, the total amount of wheel rotations is found to be 40 million.

In a corner the inner and outer wheels rotate with respect to each other. This happens because the outer wheel has to travel a larger distance than the inner wheel during cornering. Using the track width and the cornering radius the difference in rotations of the inner and outer wheels can be calculated. This amount is 2 for a 90 degree corner. Over the entire lifetime of the order picking robot this adds up to 5 million rotations.

## 2.8 Summary

- **Low cost design:** The AGV should be built out of low-cost components. The assembly should be straightforward.
- **Compact design:** The length of the AGV should be no larger than  $900 [mm]$ , and its width no larger than  $600 [mm]$ . The wheel diameter is chosen to be  $150 [mm]$  and the wheel width is chosen to be  $50 [mm]$ . The wheelbase of the AGV is therefore  $750 [mm]$ , and the track width  $550 [mm]$ .
- **Able to support the weight of the order picking robot:** Including a payload, the order picking robot weighs  $150 [kg]$ . Its center of mass then lies  $400 [mm]$  from the rear of the AGV, and  $350 [mm]$  above the floor. During standstill, the total load on the rear- and the front wheels is  $850 [N]$  and  $650 [N]$  respectively.
- **Robustness to rough floor surfaces:** The unsprung mass of the AGV should be as low as possible. The clearance between the bottom of the AGV and the floor should be at least  $30 [mm]$ .
- **Safe to use around human personnel:** The AGV should be able to come to a full stop within  $0.5 [m]$ . Tipping over of the order picking robot needs to be avoided.
- **Capable of withstanding the tire forces during travel:** The maximum acceleration of the AGV is chosen as  $4 [\frac{m}{s^2}]$ . During acceleration the load on the rear- and front wheels is  $1130 [N]$  and  $370 [N]$  respectively. The torque on the individual rear wheels during acceleration is equal to  $23 [Nm]$ . The maximum deceleration of the AGV is chosen as  $7 [\frac{m}{s^2}]$ . During deceleration the load on the rear- and front wheels is  $360 [N]$  and  $1140 [N]$  respectively. During cornering, the load on the inner and outer wheels is  $555 [N]$  and  $945 [N]$  respectively. The maximum velocity during straight line driving is  $2 [\frac{m}{s}]$ . The maximum velocity during cornering is  $1.5 [\frac{m}{s}]$ .
- **Able to remain operational for a specified lifetime:** The AGV is estimated to be operational for 10 hours a day. Its lifetime should be 5 years. The total amount of wheel rotations is determined to be 40 million. The amount of differential rotations is calculated to be 5 million.

### 3 Overall design

A warehouse features straight corridors with 90 degree corners. The robotic arm has enough degrees of freedom to compensate for a less-than-optimal positioning of the order picking robot with respect to the rack. Therefore an AGV is constructed featuring a driven differential connecting both rear wheels, and kinematically linked front wheels which can be steered. In this way longitudinal and lateral motion are decoupled. This is beneficial for maintaining velocity during cornering. To steer the AGV, an Ackermann steering linkage is designed. The AGV has four pneumatic wheels. The wheel hubs are constructed in such a way that they can be used both as rear- and front wheels. This is done to reduce the total amount of different components in the AGV, thus saving costs for individual components.

#### 3.1 Wheel force comparison

To corner, the AGV needs to accelerate laterally. Therefore the tires need to create lateral forces pointing into the corner. In the previous prototype, these forces can only be created by the rear wheels, as the casters are allowed to pivot freely. The lateral forces on the rear wheels want to rotate the AGV around its center of mass. This would mean that the AGV would steer out of the corner. To make sure that the AGV is steered into the corner instead, the rear wheels also have to create longitudinal forces to counteract the moment around the center of mass. This can be seen in the left hand side of Figure 3.1. It is more beneficial to replace the casters with wheels that are also able to create traction. In this way the forces needed for cornering are more equally distributed over the wheels.

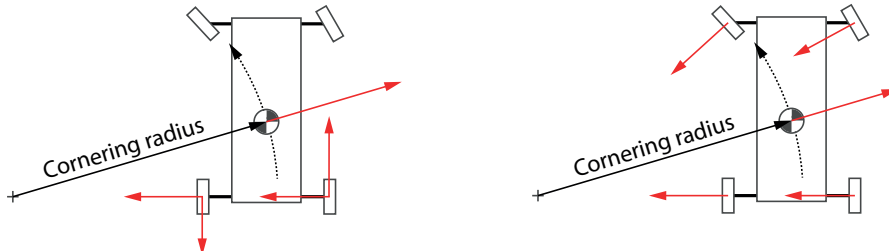


**Figure 3.1:** Force equilibrium during steady state cornering in the current prototype (left) and with rear wheel drive and front wheel steering (right)

Using rear wheel drive and front wheel steering, all the wheels can create lateral forces. This is shown in the right hand side of Figure 3.1. A comparison can be made between a tank steered AGV, and an AGV with rear wheel drive and front wheel steering, both with the same driving motor power. In that case, it is estimated that the AGV with rear wheel drive and front wheel steering can corner twice as fast as the tank steered AGV.

Because of the kinematic constraints imposed on an AGV with front wheel steering and rear wheel drive, path planning and obstacle avoidance algorithms are more complex. For this reason AGV's are usually constructed in such a way that the complexity of the software is kept to a minimum. However, this does not result in an AGV with optimal performance in warehouses with rough floors and bumps. While more complicated than software for tank steering AGV's, algorithms have been developed for self-driving cars [2][3][4][5], and similar algorithms for AGV's have been around for as early as 1993 [6].

### 3.2 Ackermann steering

When a wheel follows a circular trajectory, ideally the centerline of the wheel should intersect the midpoint of the circular trajectory. The wheel then behaves as the bottom of a cone which is rolled around its tip over a flat surface. For automobile design, this means that the centerlines of all the wheels should intersect in a single point. This point would be the center of the circular trajectory followed by the vehicle. This situation is referred to as Ackermann steering. An example of it can be seen in Figure 3.2, in dotted lines.

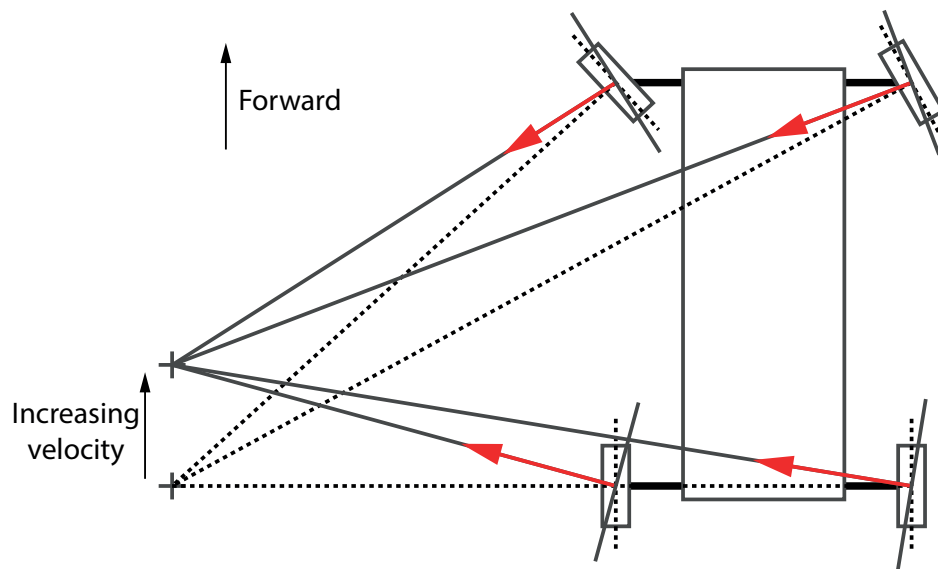


**Figure 3.2:** Schematic representation of Ackermann steering. The dotted lines represent the ideal scenario in which the centerlines of the front wheels intersect the centerline of the rear wheels. The solid lines represent a situation closer to reality, where the wheels exert lateral forces on the floor surface, and develop a slip angle. It is indicated that the center point of the circular trajectory moves forward with increasing velocity.

Lateral tire force can only be generated when the tire is slightly displaced with respect to the wheel rim. During cornering, the wheels do not roll in a direction perpendicular to their centerlines. This is referred to as the development of a slip angle[1][7]. The effect of this is represented by the solid lines in Figure 3.2. The center point of the circular trajectory moves forward with respect to the ideal Ackermann point. Ideal Ackermann steering is thus only possible at zero velocity, as the wheels need to develop a slip angle to allow the vehicle to corner. The magnitude of the lateral acceleration thus determines where the center point of the corner lies exactly. However, in vehicles where the cornering velocity is kept low, Ackermann steering is still used.

Ackermann steering can be achieved with a steering linkage as show in the left-hand side of Figure 3.3. When the wheels are pointed forwards, the steering arms connected to the wheels should lie on the lines connecting the upright of the wheel with the midpoint of the centerline of the rear wheels. The steering arms are connected by a steering link. The downside of this mechanism is that the instantaneous point of rotation moves away from the midpoint of the centerline of the rear wheels when steering. The Ackermann steering principle is followed less with greater steering angles.

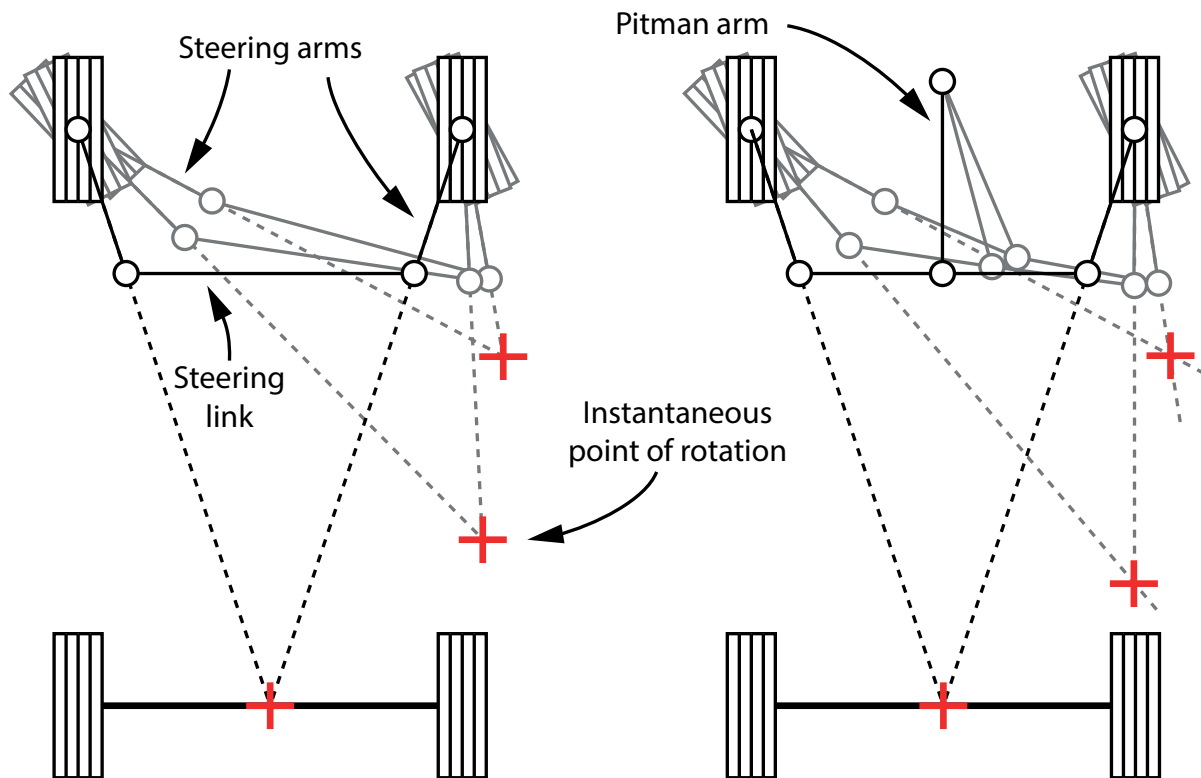


**Figure 3.3:** Left: Ackermann steering linkage. Right: Ackermann steering linkage with an added pitman arm.

The steering linkage on the left-hand side of the Figure 3.3 offers limited possibilities of actuating the steering link between the steering arms. In the right hand side of Figure 3.3 the steering linkage is complemented with an additional link. This link is called the Pitman arm. A rotation point is added around which the Pitman arm can be actuated.

In Figure 3.4 it may be observed that the addition of the Pitman changes the excursions of the steering linkage. The instantaneous point of rotation of the linkage with the pitman arm describes a curve with a broader apex than the linkage without the pitman arm. This means the Ackermann principle is followed more closely by the mechanism with the added Pitman arm. Furthermore, the Pitman allows for easier actuation of the steering linkage.

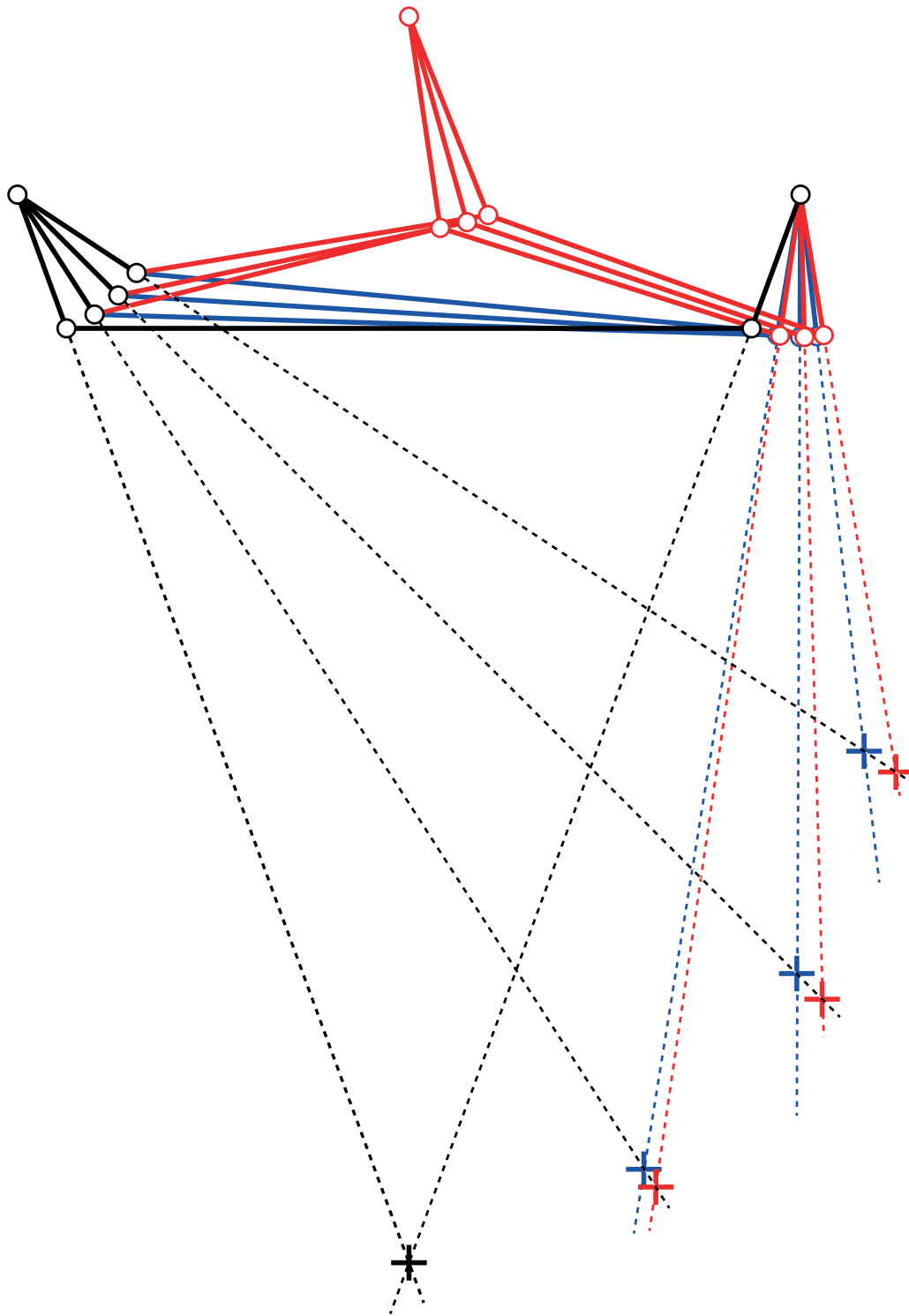


**Figure 3.4:** Comparison of the movement of the instantaneous point of rotation for the linkages shown in the left hand side (blue) and right hand side (red) of Figure 3.3

### 3.3 Tire choice

Many indoor AGV's have wheels with a solid steel wheel hub. Directly on the wheel hub a polyurethane coating is added. Such wheels offer a high load carrying capacity, which is particularly useful for AGV's that need to carry entire pallets with products. Wheels with polyurethane coatings perform well on floor surfaces with few irregularities. Compared to pneumatic wheels of the same diameter, polyurethane wheels have more mass. This increases the unsprung mass of the AGV, and makes it less useful on floor surfaces with many irregularities. Next to this, polyurethane wheels cannot generate as much traction as pneumatic wheels of the same size. Lastly, a polyurethane wheel needs to be replaced entirely when it is damaged. Pneumatic wheels can often be repaired by changing the tire. As the order picking robot does not need to carry large payloads, pneumatic wheels are therefore preferred over solid wheels.

Due to the load on the wheel, it will slightly deform, as can be seen in Figure 3.5. Rolling a loaded wheel therefore continually deforms the tire. As deforming the tire takes a certain amount of energy, energy is lost while rolling the wheel. To reduce the amount of energy lost, the wheels should either be thin and have a large diameter, or be wide and have a small diameter [1]. Wheels with a large diameter result in a heavier unsprung mass and higher torque needed on the drive shaft. Therefore tires with a radius of 150 [mm] and a width of 50 [mm] (6x2 inches) are used. Such tires are predominantly used on small scooters.

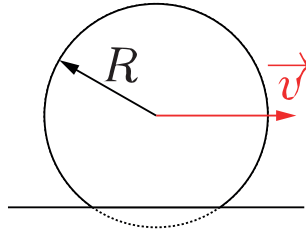


**Figure 3.5:** Deformation of a loaded wheel. The dotted line indicates the shape of the wheel before loading.

The stiffness of the tire influences the clearance between the AGV and the floor. This makes it important input for the design of both the front- and rear wheel suspension. The stiffness of a tire depends on the tire pressure. A typical value for the tire stiffness of a pneumatic wheel is  $170 \left[ \frac{N}{mm} \right]$ , at a tire pressure of 2[bar] [8]. While the chosen tires can be inflated up to 5[bar], this value gives a rough indication for the loss in clearance using a pneumatic tire. During acceleration, the load is equal to 570 [N] per wheel. The indentation of the tire can now be calculated:

$$\frac{570 [N]}{170 \left[ \frac{N}{mm} \right]} \approx 3.5 [mm]$$

This can be used to determine the necessary clearance between the rear wheel suspension and the floor.

### 3.4 Wheel construction

The construction of the wheel is shown in Figure 3.6. A hub reinforcement is welded onto each half of the wheel hub. These hub reinforcements have internal flats. The flats allow a drive shaft with equally sized flats to transmit torque to the wheel hub. The tube and the tire are put over the inner wheel hub. The air nipple of the tube is put through holes in the rim of the inner wheel hub as well as the side of the inner wheel hub. The outer wheel hub is then aligned with the inner wheel hub. The air nipple should go through the hole in the side of the outer wheel hub. It can then be accessed from the side of the wheel, where it allows for inflation of the inner tire. The inner and outer wheel hub are bolted together using six bolts and nuts. This bolted construction allows for replacement of both the inner and outer tires in case they have been punctured.

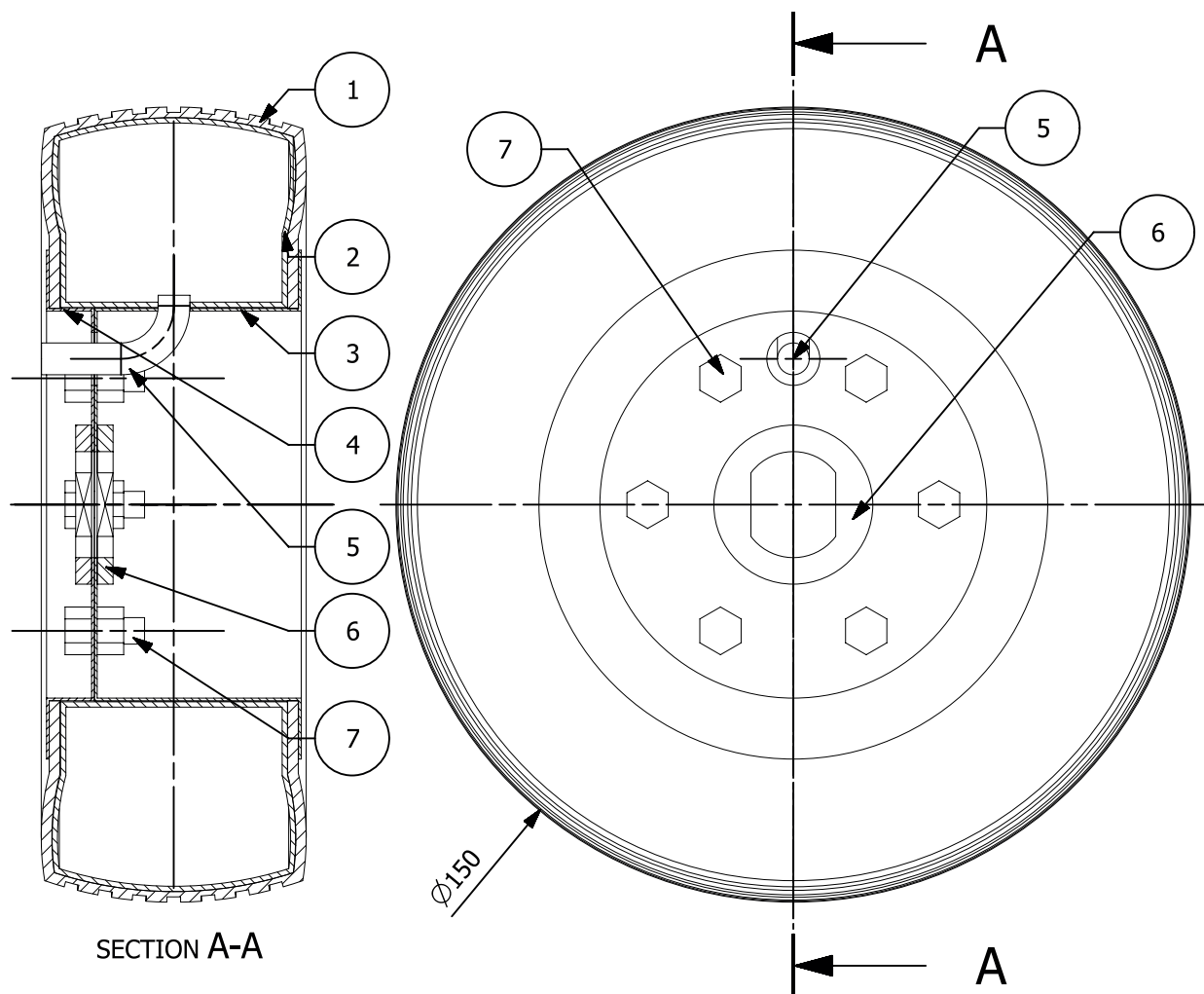


**Figure 3.6:** Construction of the Wheel. ①: Tire ②: Tube ③: Outer wheel hub ④: Inner wheel hub ⑤: Air nipple ⑥: Hub reinforcement ⑦: Bolt



## 4 Front wheel suspension

An overview of the front wheel suspension is presented in Figure 4.1. It is based on the McPherson strut suspension design. This design was chosen for its compactness and straightforward assembly. A leaf spring is attached to the bottom of the upright with a ball joint. Dampers are connected to the upright from the top. The upper part of the dampers should be attached to the frame. The centerlines of the dampers point to the ball joints attached to the leaf spring. The piston of the dampers can be freely rotated. This allows the wheels to be steered around the centerline of the damper. A steering arm is added to the upright, allowing the steering of the wheel to be actuated. The wheel is therefore constrained in 4 degrees of freedom; only the rotation of the wheel around its axis and upward motion of the wheel are free.

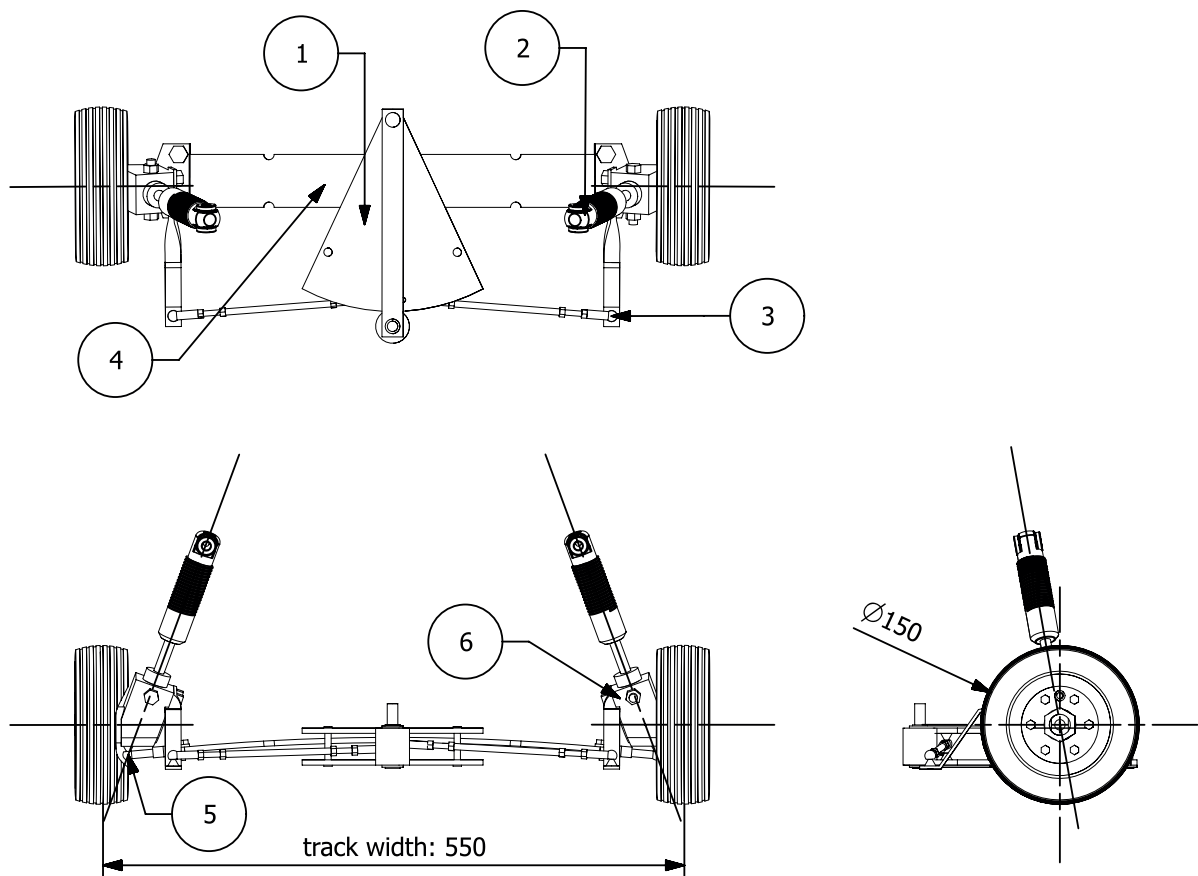


**Figure 4.1:** Front wheel suspension. ①: Pitman arm ②: Damper ③: Steering arm ball joint ④: Leaf spring ⑤: Upright ball joint ⑥: Upright

## 4.1 Construction of the upright

The wheel is attached to the front wheel suspension via the upright, shown in Figure 4.2. The wheel is mounted on an axlestub. A more detailed view of this axlestub is shown in Figure 4.3. The upright contains two deep groove ball bearings, which are positioned at an equal distance from the midline of the wheel hub. As the normal load acting on the wheel is introduced into the axlestub via the hub reinforcements, a moment arises in the middle of the ball bearing closest to the wheel hub reinforcements. A second ball bearing therefore needs to be used, as the normal load acting on the wheel would otherwise load the ball bearing close to the wheel hub reinforcements unfavorably. The inner races of the bearings are kept apart by the bearing spacer. The axlestub rests against the inner race of the bearing farthest from the hub reinforcements. Another spacer is used to keep the hub reinforcement and the inner race of the bearing closest to the hub reinforcement apart. The flats of the axlestub are aligned with the flats in the hub reinforcement, and a locknut is put over the end of the axlestub. The inner races of the bearings are hereby pulled against the hub reinforcement.

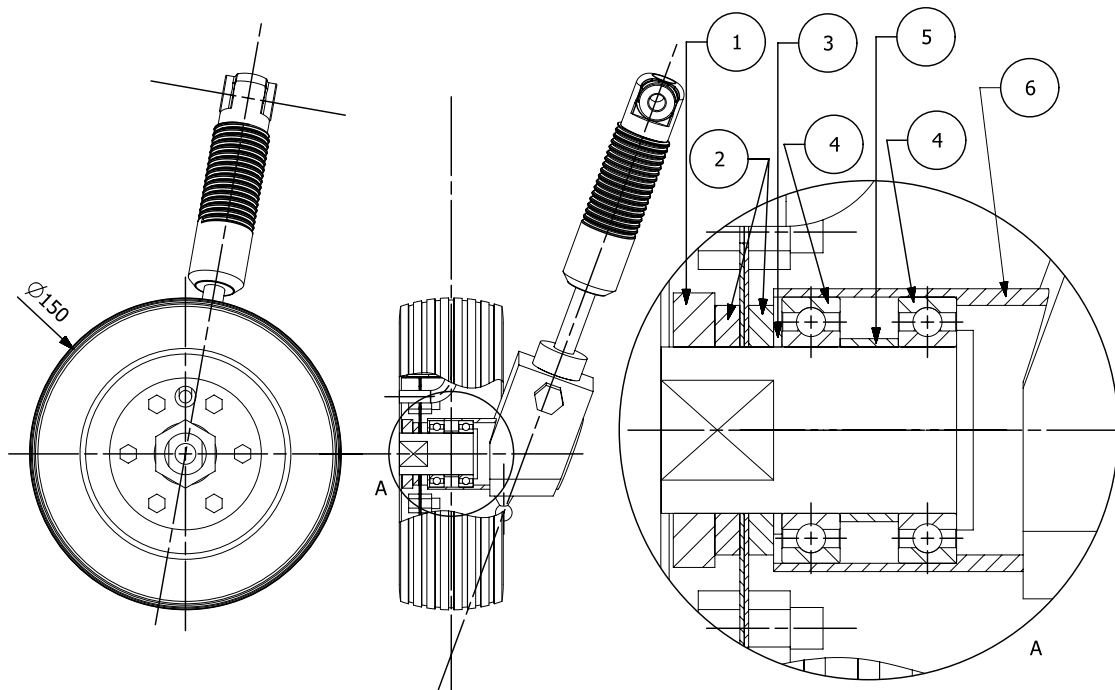


**Figure 4.2:** Upright. ①: Locknut ②: Hub reinforcement ③: Spacer ④: Ball bearings ⑤: Bearing spacer ⑥: Upright

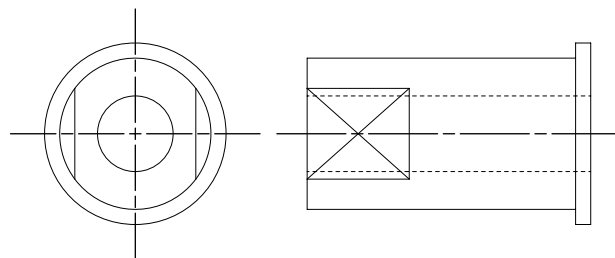


**Figure 4.3:** Detailed view of the axlestub used in the front wheel

## 4.2 Pitman arm

The pitman arm is placed over the leaf spring. A detailed view of the Pitman arm is shown in Figure 4.4. The Pitman arm is made using a sandwich of two identical partial plastic gears. The ball joints of the rods connected to the steering arms are directly attached to these gears. The gears are separated by bushes, which also serve as an end stop for the mechanism. This prevents the gears from losing contact with the pinion, as can be seen in Figure 4.5. The pitman arm is connected to the bottom of the frame of the AGV. A motor contained inside of the frame can therefore drive the pinion running over the partial plastic gears. The Pitman arm is connected to the steering arms with the steering links. This can be seen in Figure 4.6.

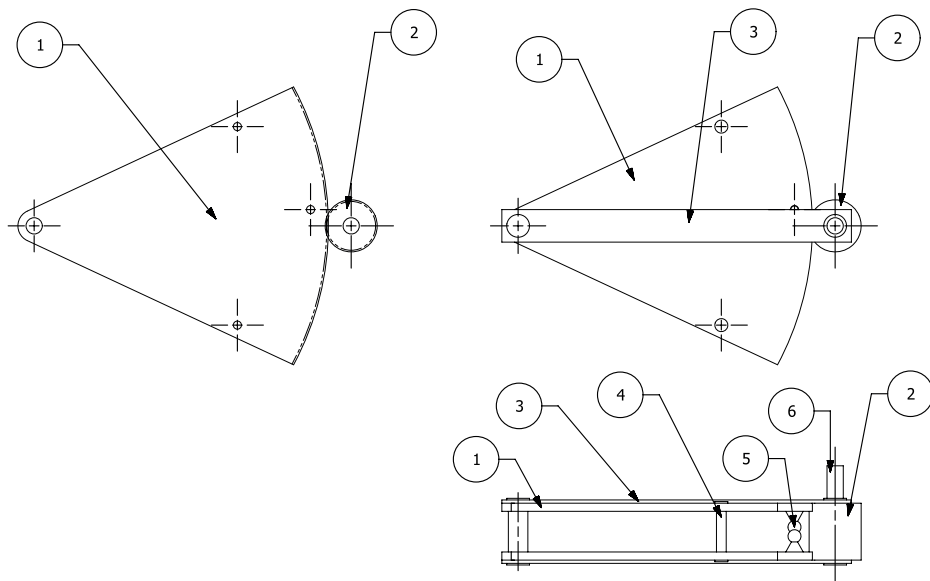


**Figure 4.4:** Detailed view of the Pitman arm (1): Partial gear (2): Driving pinion (3): Sandwich plate (4): Bush/ end stop (5): Ball of ball joint (6): Driven axle

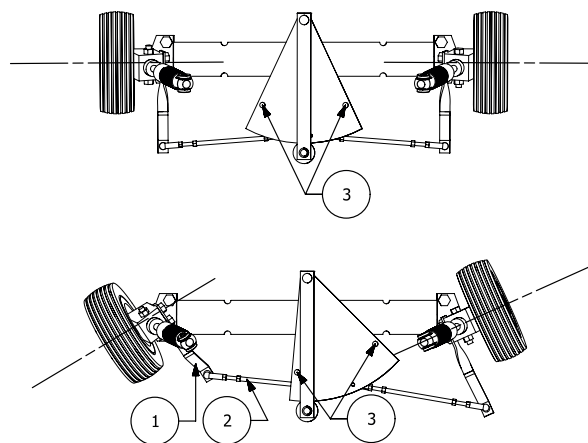


**Figure 4.5:** Excursion of the steering mechanism (1): Steering arm (2): Steering link (3): Bush/ end stop

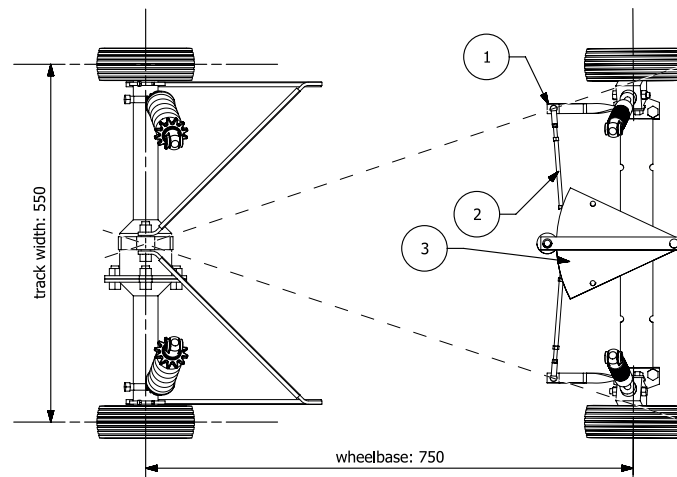


**Figure 4.6:** Placement of the steering mechanism. The lines extended between the ball joint of the steering arm and the upright intersects the centerline of the rear axle in the middle (1): Steering arm (2): Steering link (3): Pitman arm

### 4.3 Leaf spring

A partial view of the assembled leaf spring can be seen in Figure 4.7. The leaf spring is attached to the bottom of the frame of the AGV. A block is attached to the free end of the leaf spring. This block is used to attach the cup of a ball joint to the leaf spring. This cup will contain the ball connected to the upright.

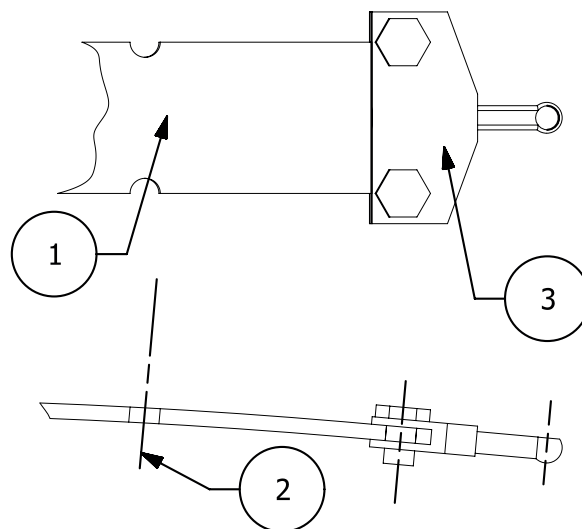


**Figure 4.7:** Assembly of the leaf spring. (1): Leaf spring (2): Attachment to frame (3): Block containing cup of ball joint

Because the AGV drives over irregularities in the floor surface, the leaf spring constantly deforms elastically. The leaf spring itself is therefore fabricated from a straight strip of spring steel. This type of steel is used because of its high endurance limit. The leaf spring will be attached to the block containing the ball joint and the silent blocks using partial holes in the side of the leaf spring. This can be seen in Figure 4.8. Drilling holes into the leaf spring would result in stress concentrations, which can lead to failure of the

spring. When the AGV needs to make an emergency stop, most load is transferred to the front wheels. In this situation, the leaf spring needs to be perfectly straight. The high longitudinal forces caused by deceleration would otherwise twist the leaf spring, and thus lead to unnecessary stress concentrations. The leaf spring is therefore given a slight radius downwards. The radius should be chosen in such a way that it closely resembles the shape of an initially flat leaf spring which is subjected to the normal load on the wheels during full deceleration.

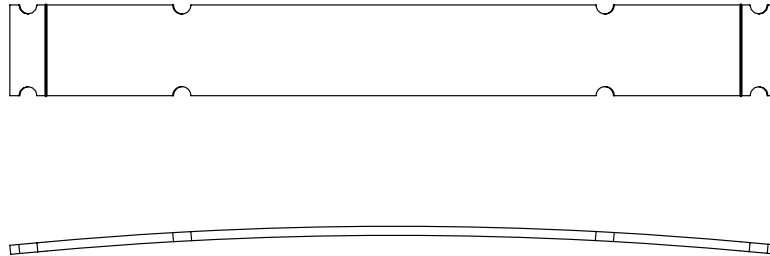


**Figure 4.8:** Leaf spring curvature.

## 5 Rear wheel suspension

The rear wheel suspension is based on the suspension system of a truck. It features a mechanical differential contained in a rigid axle. The axle is mounted to the frame using an A-frame, two longitudinal struts and two shock absorbers. An overview of the rear wheel suspension can be found in Figure 5.1.

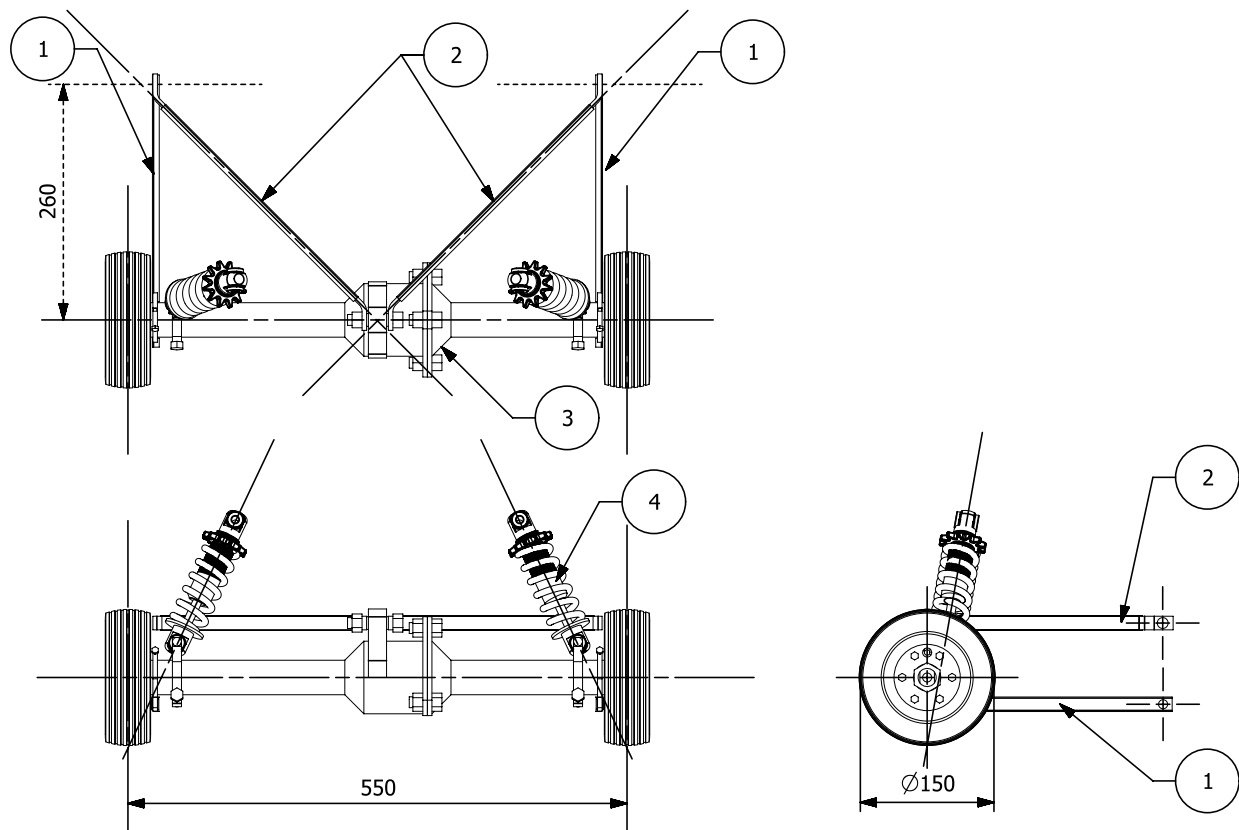


**Figure 5.1:** Overview of the designed rear wheel suspension. (1): Strut (2): A-frame (3): Differential housing (4): Shock absorber

### 5.1 Rear wheel drive and suspension concepts

A rear wheel suspension housing an electronic differential, a mechanical differential using Nylon gears and a mechanical differential using steel gears are conceptualized in individual subsections. A concept choice is made using the advantages and disadvantages listed with each concept.

#### 5.1.1 Electronic differential

In Figure 5.2 a rear wheel drive concept based on an electronic differential is shown. It features two electric motors independently driving the rear wheels. When the AGV is steered into a corner, the motor controllers should therefore force the electric motors to spin the inside and outside wheels at the correct rotational velocity. The drive shaft is contained in an axle, and directly connects the wheel to the electric motor. The axle is attached to the AGV using a leaf spring close to the center of the AGV. The axle is also

attached to the frame using a longitudinally placed strut. This strut is connected to the bottom of the axle, near the wheels. Together, the leaf spring and the strut constrain longitudinal motion and rotation around the normal to the floor surface. Rotation around the centerline of the AGV is free, which allows vertical motion of the wheel during a bump.

The electric motors are contained in a thick-walled tube with saw cuts. The saw cuts create an internal degree of freedom in the tube. When the tube is sandwiched between the leaf springs, the internal degree of freedom of the tube allows the rotation of the wheels around the centerline of the AGV. The thick-walled tube couples the rotation around the centerline of the AGV of both axles. Therefore, when the normal load on one wheel increases, both wheels move up. The thick-walled tube is attached to an A-frame, above the centerline of the axles. This A-frame constrains the lateral movement of both wheels. As the A-frame and the struts are attached above and below the axle respectively, they constrain the rotation around the centerline of the axle. The weight of the frame is carried by shock absorbers. The centerlines of the shock absorbers point at the contact patch between the wheels and the ground, in order to introduce the normal load acting on the wheels properly into the frame of the AGV.

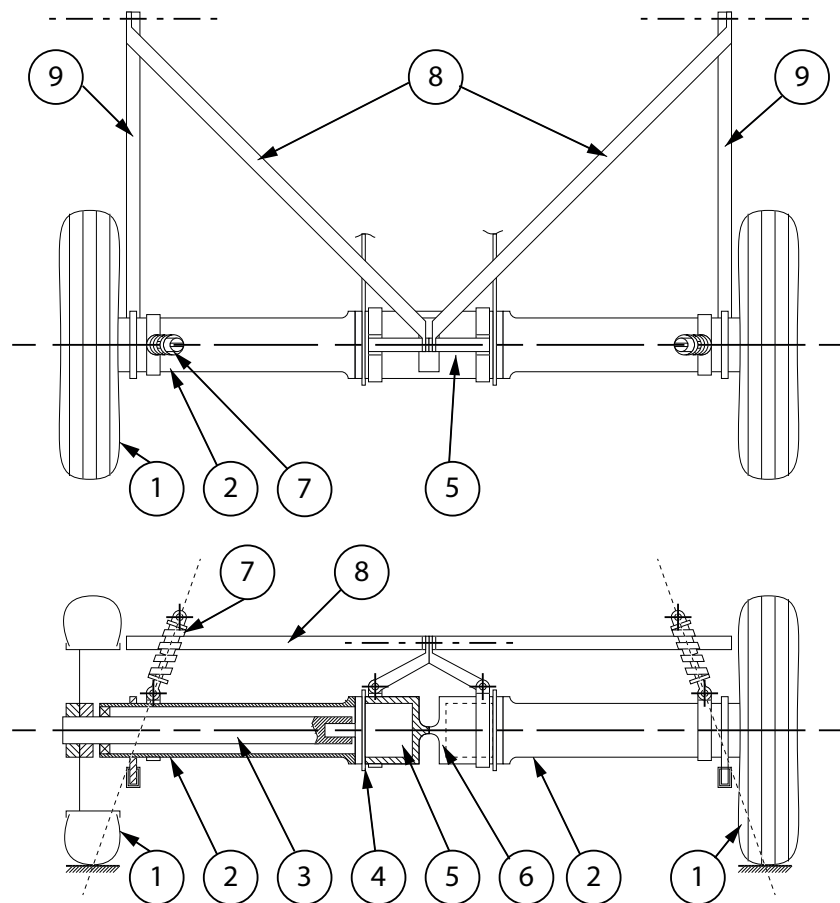


**Figure 5.2:** Concept of a rear-wheel drive with an electronic differential. (1): Wheel (2): Axle (3): Shaft (4): Leaf spring (5): Electric motor (6): Thick-walled tube with saw cut (7): Shock absorber (8): A-frame (9): Strut

Employing the described electronic differential concept has the following advantages (+) and disadvantages (-):

- + Independently driving the rear wheels allows for skid steering maneuvers. This can be used to reduce the minimum cornering radius of the AGV.
- + The thick-walled tube makes sure that the frame does not roll much when load is transferred from one wheel to the other, for example during cornering.
- Because the motion of both axles is coupled with the thick-walled tube, the unsprung mass felt by a single wheel is the total weight of the rear suspension.
- The behavior of the AGV is unpredictable when one of the electric motors fail.
- The size of the electric motor directly influences the clearance between the floor and the bottom of the AGV.

### 5.1.2 Mechanical differential using Nylon gears

A mechanical differential can be made out of Nylon gears. Using Nylon gears instead of steel gears has the following advantages [9]:

- Nylon gears cost less than steel gears
- No lubrication is needed when Nylon gears are paired with steel pinions
- Nylon gears run more smoothly and more silently compared to steel gears

Nylon is less strong than steel. Therefore it is beneficial to reduce the tooth forces on the Nylon gear as much as possible. For the gears in the differential, this can be done by adding a reduction close to the wheels, as can be seen in Figure 5.3. The diameter of the gear of the reduction close to the wheels is constrained by the required clearance between the bottom of the AGV and the floor. Taking into account the wheel radius, the indentation of the wheels, and saving room for a housing for the reduction, a reference diameter of  $\text{Ø}65 [mm]$  is chosen for the gear of the reduction. The tooth forces on the gears will be calculated using the maximum torque during acceleration. As the AGV will not constantly accelerate during its lifetime, this ensures that the reductions last for the entire lifespan of the AGV. The teeth forces are calculated:

$$\frac{23 [Nm]}{0.0325 [m]} \approx 710 [N]$$

A close estimation of the necessary size of the gear can be made by using the following equation:

$$S = \frac{\vec{F}_{tooth}}{MBY}$$

In which  $S$  is the fatigue stress,  $\vec{F}_{tooth}$  is the force on an individual tooth,  $M$  is the module of the gear,  $B$  is the width of the gear and  $Y$  is the *Lewis form factor*. The fatigue stress  $S$  is a parameter that depends on the material and the estimated amount of load cycles. The design stress for Nylon gears can be determined using the characteristic in Figure 5.4. The Lewis form factor depends on the exact shape of the teeth of a gear. For a first estimation  $Y$  should be chosen as 0.6 [9].



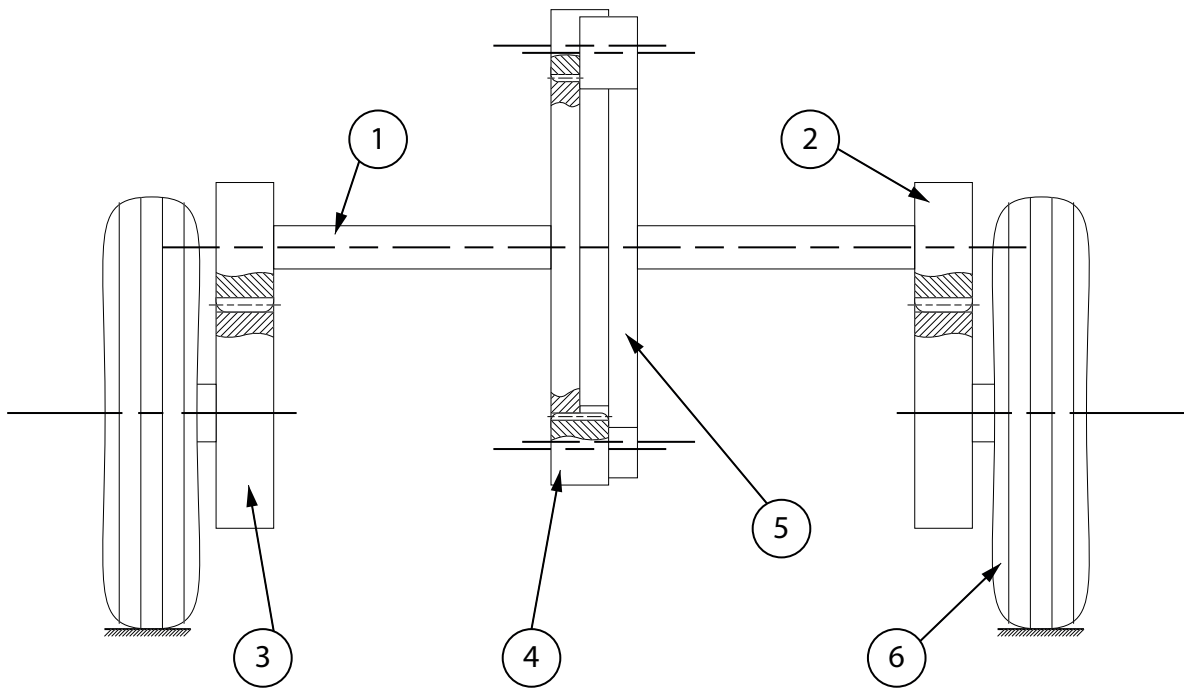


**Figure 5.3:** Drivetrain using a Nylon mechanical differential. ①: Drive shaft ②: Steel pinion ③: Nylon gear ④: Steel pinion of spur gear differential ⑤: Nylon gear of spur gear differential ⑥: Wheel

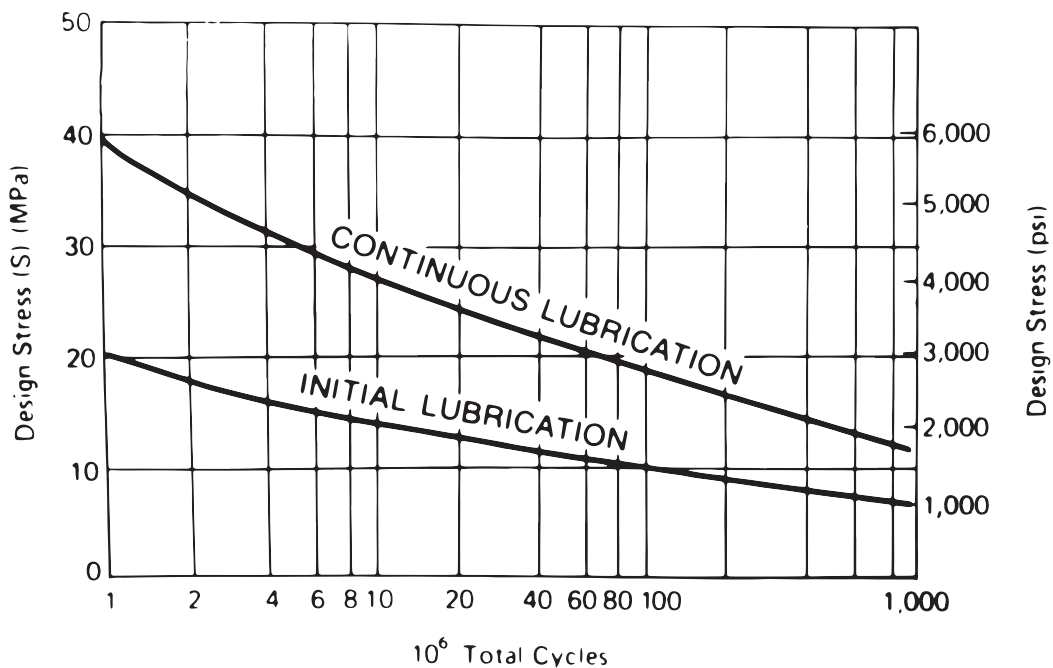


**Figure 5.4:** Fatigue stress characteristic of Nylon. The fatigue stress is plotted versus the estimated total amount of load cycles.

The Nylon gear is paired with a steel pinion, and does not need continuous lubrication. Therefore the curve for initial lubrication is used. The total amount of wheel rotations during the lifetime of the AGV is equal to 40 million. The corresponding fatigue stress is  $S = 10 [MPa]$ . As the tooth forces on the Nylon gear are relatively high, a module of  $M = 5 [mm]$  is chosen. The width of the gear can now be calculated:

$$\frac{710}{5 \cdot 10 \cdot 0.6} \approx 25 [mm]$$

Choosing a steel pinion with a reference diameter of  $\varnothing 30 [mm]$  results in a reduction of approximately 1:2. The reduction cannot be made larger as the a module of  $M = 5 [mm]$  prohibits the use of a smaller reference diameter of the pinion. With this reduction the torque on the driving axle is reduced to approximately  $12 [Nm]$ . This is again a worst case scenario calculation, as the AGV will not accelerate the entire time. It is chosen to design a spur gear differential. A schematic drawing of such a differential can be seen in Figure 5.5. A spur gear differential is less costly than a bevel gear differential or a Torsen differential. This is because spur gears are easier to manufacture. The drive shaft is located above the wheel axes. This allows for a reference diameter of  $\varnothing 120 [mm]$  for the gears of the spur gear differential. The gears can then be used in combination with pinions having a reference diameter of  $\varnothing 20 [mm]$ . The torque is distributed over two pinions. This is in order to balance the differential during its rotation. The tooth forces can be calculated as follows:

$$\frac{1}{2} \cdot \frac{12 [Nm]}{0.060 [m]} \approx 100 [N]$$

The gears of the differential rotate 5 million times with respect to each other over the course of the AGV's lifespan. This results in 10 million load cycles because of the use of 2 pinions. As the steel pinions interact with each other, lubrication should be added to the differential. Because the total amount of load cycles is low compared to the total amount of wheel rotations, continuous lubrication is not necessary. The fatigue stress is therefore  $S = 15 [MPa]$ . A module of  $M = 1 [mm]$  is chosen for a smooth operation. The width of the gears in the spur gear differential can now be calculated:

$$\frac{100}{1 \cdot 15 \cdot 0.6} \approx 10 [mm]$$

The width of the pinions chosen twice as large. This results in the spur gear differential shown in Figure 5.5.

A straightforward way of housing the components of the drivetrain is shown in Figure 5.6. Tubes are used to connect the output ends of the reductions with each other. The tubes around the centerline of the wheels and the centerline of the differential are connected to each other using plates. Therefore, lateral forces exerted by the wheels on the construction do not bend the housing of the reduction. Suspension links connect the reduction housing and the differential housing to the frame of the AGV. An A-frame can be attached to the top of the differential housing. The A-frame constrains lateral motion of the housing. Struts are attached to the bottom of the tube around the wheel centerline. The struts constrain the rotation around the normal to the floor. Together, the struts and the A-frame constrain longitudinal motion and the rotation around the centerline of the wheels. Vertical motion, and rotation around the centerline of the AGV are left free.

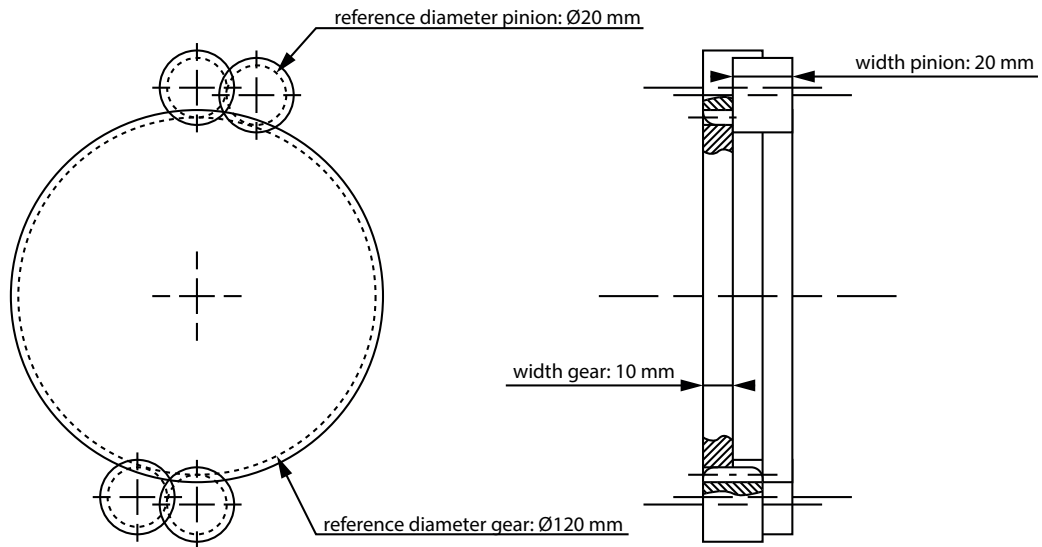


**Figure 5.5:** Schematic drawing of the designed Nylon spur gear differential

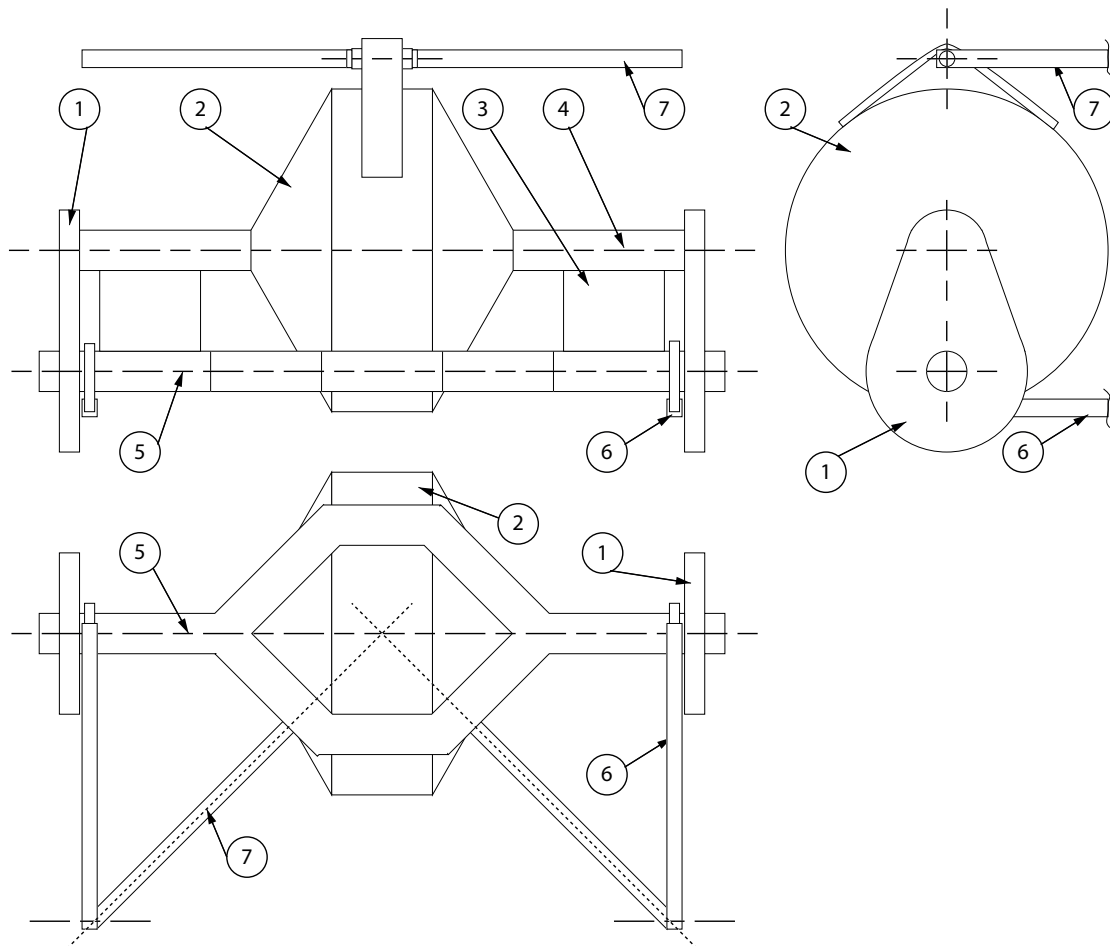


**Figure 5.6:** Housing for the Nylon reduction and spur gear differential. ①: Reduction housing ②: Differential housing ③: Plate ④: Drive shaft centerline ⑤: Wheel centerline ⑥: Strut ⑦: A-frame

Employing the concept of a mechanical differential made using Nylon gears has the following advantages (+) and disadvantages (–):

- + The differential could be driven with a chain or a belt. Because of the large diameter of the differential, and the reduction close to the wheels, a small sprocket attached to the driving motor results in a large reduction between the motor and the wheels. Therefore expensive gear sets do not have to be installed on the driving motor.
- + Moving the drive shaft upwards using the reduction at the wheels results in a large clearance between the floor and the bottom of the AGV.
- The complex shape of the differential housing and the reduction housing makes the concept costly.
- The size of the housing will result in a large unsprung mass.

### 5.1.3 Mechanical differential using Steel gears

A mechanical differential can also be made using steel gears. Steel is strong enough to allow for the direct connection of the drive shafts to the gears of the spur gear differential. A concept featuring such a drivetrain is visualized in Figure 5.7. The differential and the drive shafts are enveloped in the axle. An A-frame and two struts are used to connect the axle to the frame. Together they constrain the axle in four degrees of freedom; only vertical motion and rotation around the centerline of the AGV are left free. Two shock absorbers are used to carry the weight of the frame.

The fatigue stress characteristic of steel remains constant above a certain amount of cycles. This is referred to as the endurance limit. Using the endurance limit, a differential can be designed which could in theory remain operational forever. Unhardened mild steel spur gears are used to construct a spur gear differential. The endurance limit of mild steel is approximately  $200 [MPa]$ .

Keeping the indentation of the wheels and the minimum clearance between the bottom of the AGV and the floor into account, the maximum diameter of the axle can be  $\text{Ø}80 [mm]$ . Saving room for a differential housing, the reference diameter of the gear is chosen to be  $\text{Ø}40 [mm]$ . The reference diameter of the pinions is chosen to be  $\text{Ø}15 [mm]$ . The torque on the drive shafts is distributed over two pairs of meshing teeth, as there are two pinions on the circumference of the gear. The maximum tooth forces can now be calculated:

$$\frac{1}{2} \cdot \frac{23 [Nm]}{0.020 [m]} \approx 580 [N]$$

Choosing a module of  $M = 1 [mm]$ , the width of the gears can now be calculated. The width of the pinions is chosen twice as large as the width of the gears.

$$\frac{580}{1 \cdot 200 \cdot 0.6} \approx 5 [mm]$$

A schematic drawing of the resulting spur gear differential can be seen in Figure 5.8. The spur gear differential fits within a diameter of  $\text{Ø}72 [mm]$ . This leaves enough room for fitting a differential housing within the axle.

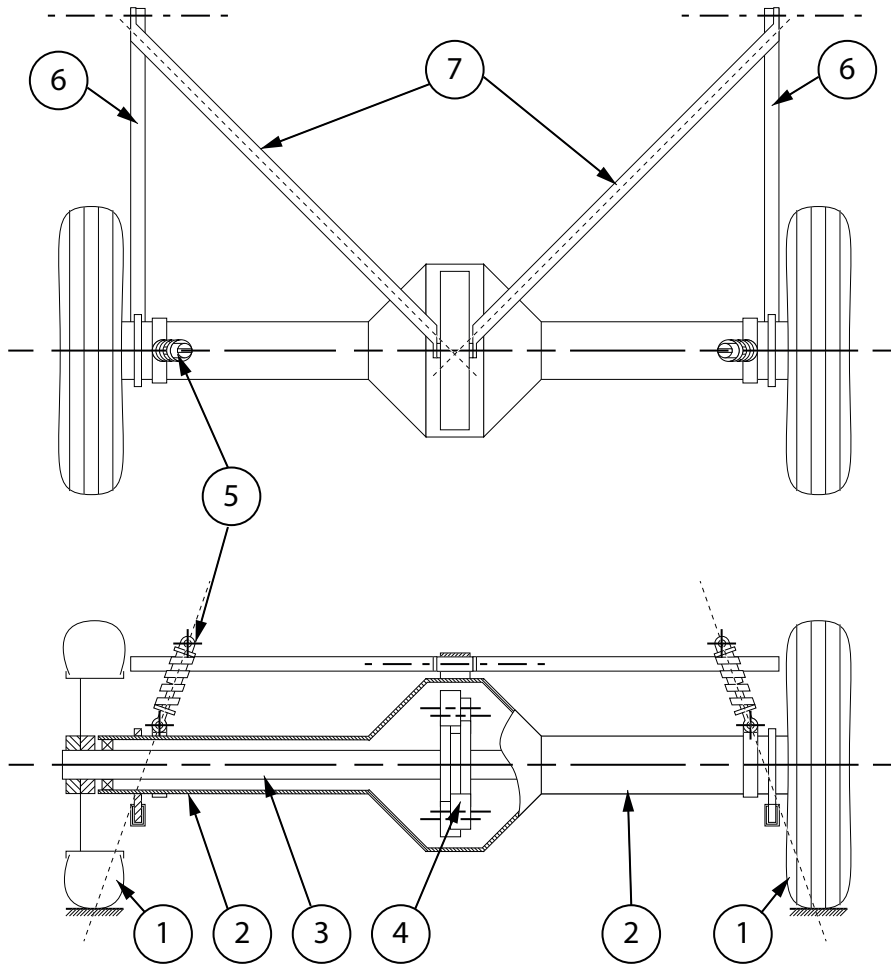


**Figure 5.7:** Drivetrain using a mechanical differential made out of steel, and corresponding suspension design. ①: Wheel ②: Axle ③: Drive shaft ④: Steel spur gear differential ⑤: Shock absorber ⑥: Strut ⑦: A-frame

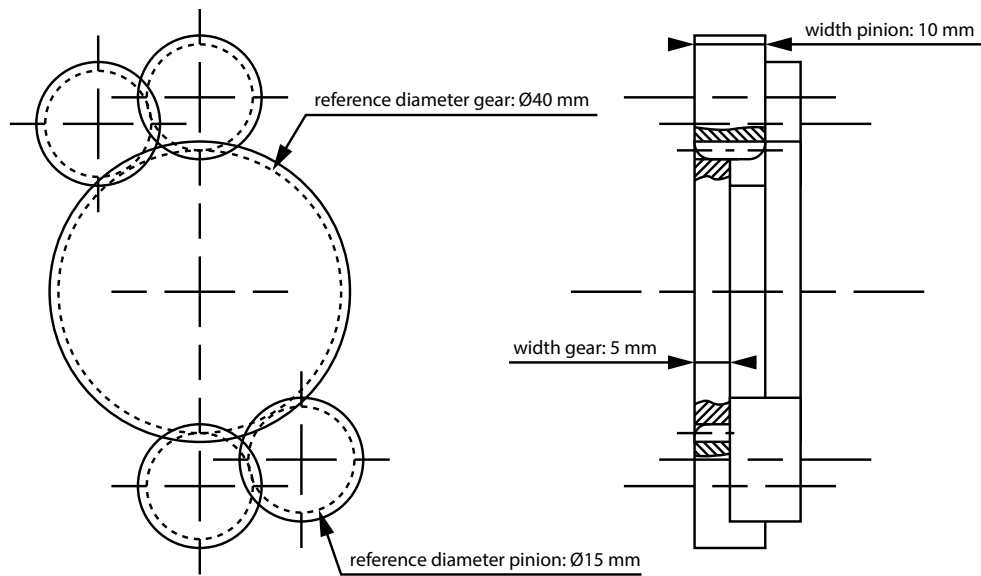


**Figure 5.8:** Schematic drawing of the designed steel spur gear differential

Employing the concept of a mechanical differential made using steel gears has the following advantages (+) and disadvantages (–):

- + The differential has a practically infinite lifetime.
- + The unsprung mass is low compared to the other concepts.
- There is little clearance between the bottom of the AGV and the floor.

#### 5.1.4 Concept choice

The concept with the steel mechanical differential is chosen over the other concepts. It can be built lightweight in comparison with the other concepts. The electronic differential offers extra maneuverability due to the possibility of skid steering, but this is not necessary as the robotic arm omits the need for more accurate positioning of the AGV. For the concept with the steel differential, this can be improved by choosing stiffer springs. Having a large reduction between the driving motor and the wheels, which can be achieved with the Nylon spur gear differential concept, is less beneficial than a low unsprung mass. As the concept with the Nylon spur gear differential has a large unsprung mass due to the size of the differential housing, it is therefore not suitable for the design of the AGV. The concept with the steel differential has a low clearance between the bottom of the AGV and the floor. However, calculations show that it is possible to maintain the minimum clearance while providing enough room for the differential.

## 5.2 Differential construction

The differential is constructed according to Figure 5.9. The differential housing contains two Nylon covers on either side of the differential itself. These covers have a center hole to accommodate the drive shaft. The cover also contains halfway holes in which the pinion axles rest. Spacers make sure that the pinions stay on the correct side of the differential.

By choosing a self-lubricating Nylon the covers can also serve as plain bearings for the drive shafts and the pinion axles. The covers are glued into the differential housing to avoid lubricant from escaping. Two indentations are made in the differential housing on either side of the Nylon covers upon assembly. It is therefore possible to transmit torque from the sprocket, through the housing, to the Nylon covers. The torque is then transmitted through the plain bearings, into the pinion axles, and into the pinions. Flats are ground onto the drive shafts to allow them to transfer torque to the wheels. The ends of the shafts also have thread to allow a locknut to be mounted on the shafts.

An aligning pin is added between the two driving shafts. This pin makes sure that the meshing of the gears remains straight. Holes are bored axially into the drive shafts. These holes contain needle bearings that guide the aligning pin. Drawn cup needle bearings are chosen for their high loading capacity, compact size and low price.

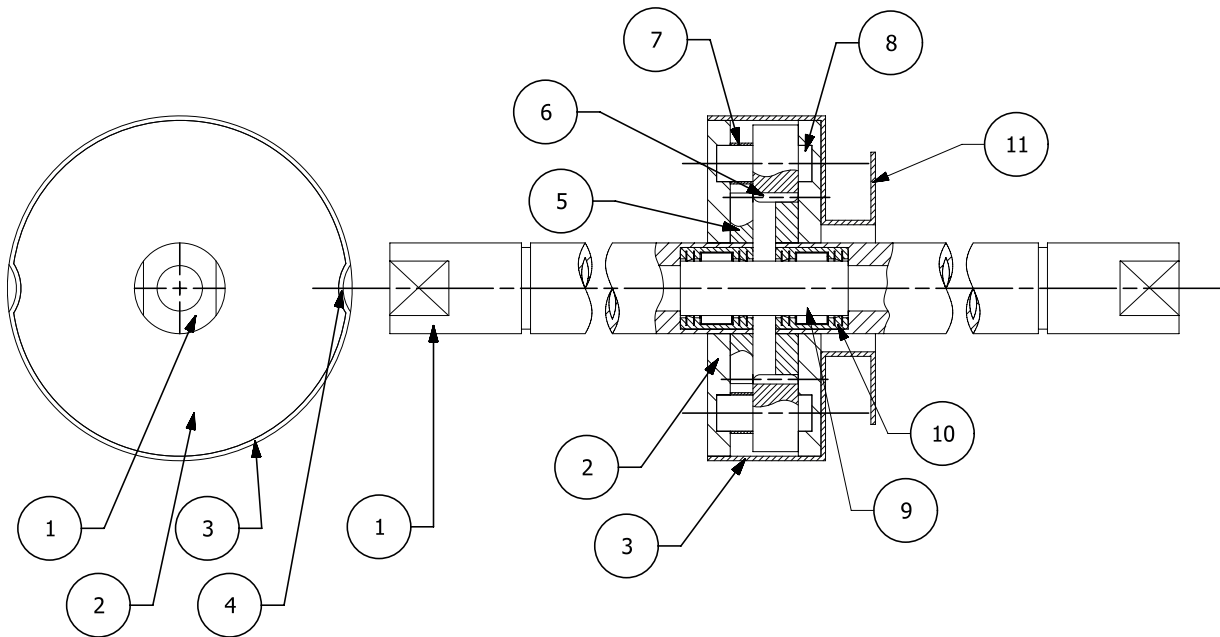


**Figure 5.9:** Figure 1: Construction of the differential plus housing. (1): Drive shaft with flats (2): Nylon cover (3): Differential housing (4): Indentation in the plastic cover/differential housing (5): Gear (6): Pinion (7): Spacer (8): Pinion axle (9): Aligning pin (10): Needle bearing (11): Sprocket

### 5.3 Axle assembly

In Figure 5.10 a section view of the rear axle is shown. The axle consists of two parts which can be bolted together using flanges. Circlips are added to the drive shafts. The drive shafts are put through deep-groove ball bearings which are contained within the axles, close to the wheels. Deep groove ball bearings can handle lateral forces, and are lower in cost compared to angular contact ball bearings. Next to this the mounting tolerances for deep-groove ball bearings are less critical than for angular contact ball bearings. A spacer is added over the drive shaft, whereafter the wheel hub is aligned with the flats on the shaft. Using a locknut, the inner race of the ball bearing is pulled against the spacer, which rests against the wheelhub. Lateral forces from the wheels in either direction can now be transmitted through the ball bearing. The ball bearing lies exactly on the midline of the wheel. This ensures that vertical forces are correctly introduced into the ball bearing. The ball bearing transmits the wheels forces into the axle, where the suspension links and the shock absorbers can transmit them into the frame.

Flanges are attached to both halves of the axle. A schematic view of these flanges can be seen in Figure 5.11. The flanges can be cut from a plate, and welded to the individual axle halves. When the drive shafts and the differential are assembled in the axle, the flanges are bolted together, joining both axle halves together.

In Figure 5.13 the mounting points for the struts and the A-frame are shown. Mounts for the struts could be directly attached to the individual halves of the axle. However, this would result in strict tolerances for the individual axle halves, as an offset strut mount

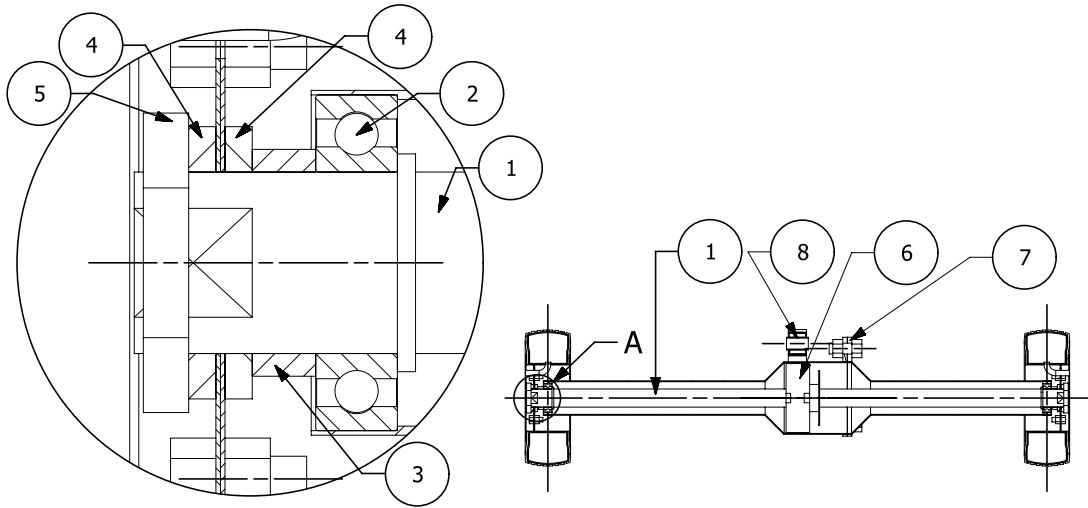


**Figure 5.10:** Section view of the rear axle. (1): Drive shaft (2): Deep groove ball bearing (3): Spacer (4): Hub reinforcement (5): Locknut (6): Differential (7): Flange (8): A-frame mount

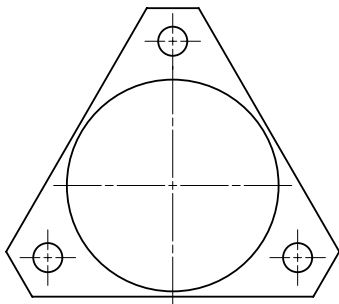


**Figure 5.11:** Flange mounted on both axle halves.

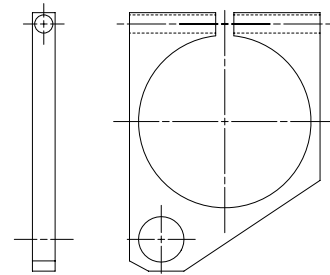


**Figure 5.12:** Mounting clamp for the struts.

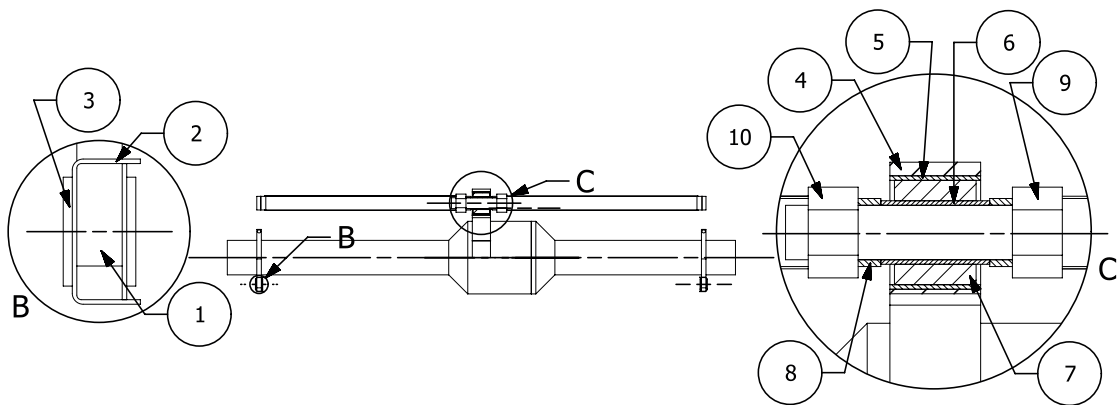


**Figure 5.13:** Mounting points for the strut and the A-frame on the axle. (1): Strut clamp (2): Strut (3): Bolt (4): Silent block bracket (5): Outer tube of silent block (6): Inner tube of silent block (7): Vulcanized rubber between the inner and outer tube of the silent block (8): A-frame (9): Bolt (10): Nut



could hinder the suspension travel. Strict tolerances would also make the production of the axle halves more expensive. Therefore clamps are used to attach the struts to the axle. Such a clamp is shown in detail in Figure 5.12. The axle runs through the large central hole of the clamp, and a bolt is screwed into the clamp to tighten it around the axle. A strut can be attached to the clamp using a bolt. The A-frame is mounted to the axle by use of a silent block. A silent block consists of an inner and an outer tube with vulcanized rubber in between. It offers some damping, as well as minor rotations of the inner tube with respect to the outer tube in three directions ( $\leq 5^\circ$ ). Both halves of the A-frame are attached to the silent block using a bolt and a nut.

#### 5.4 Construction of the A-frame and the struts

The struts and the A-frame are fabricated by bending strips in a U-shape, and welding a straight strip inside, as can be seen in Figure 5.14. For the A-frame, also angled inserts are welded in both ends of the tube to allow the halves of the A-frame to be attached to the axle under an angle. The struts are created in a similar fashion, the only difference being that no inserts are welded into them. Because the ends of the struts are left open, they are torsionally compliant. This is necessary in order to allow for the rotation of the axle around the centerline of the AGV.

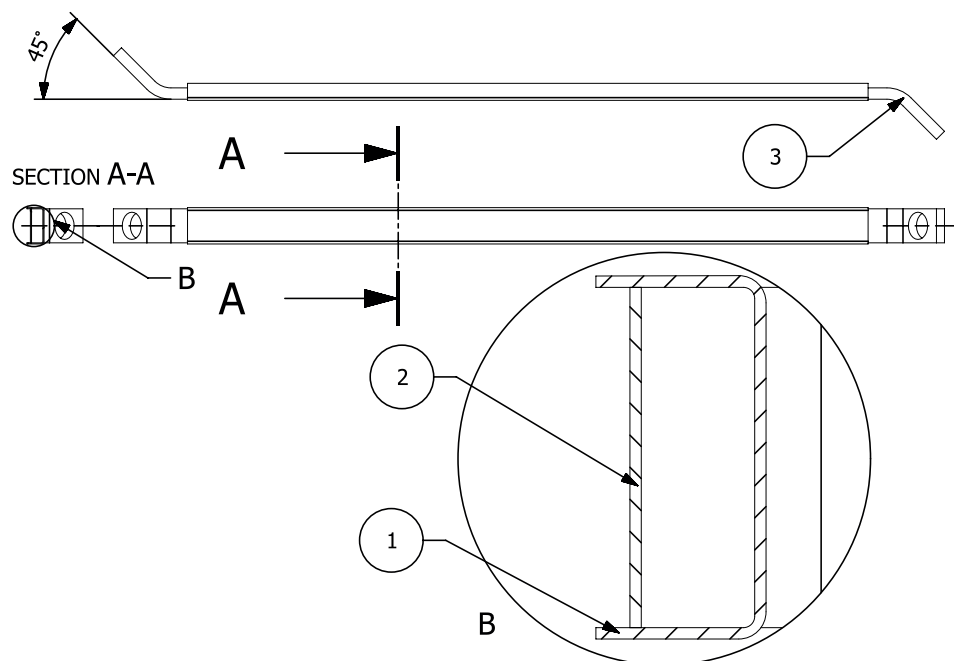


**Figure 5.14:** Construction of one half of the A-frame. (1): Bent strip (2): Straight strip (3): Angled insert

## 6 Conclusion

A front- and rear wheel suspension design was made for an AGV that needs to support an order picking robot. Both front- and rear wheel suspension are designed to enable the AGV to corner faster than the current AGV allows the order picking robot to, and to be more robust to irregularities in the floor surface. Next to this, cost effectiveness for the production of components and assembly of the AGV is taken into account.

The new AGV has rear wheels drive, and front wheel steering. Separating the actuation for driving and steering decouples the motion control of the AGV. This makes it easier to maintain velocity during cornering. The steering is based on an Ackermann steering linkage. Pneumatic wheels are used on the AGV, which are lighter than commonly used polyurethane wheels. The wheel hubs have been constructed so they can be used both as front and rear wheels. This decreases the component count of the AGV.

The front wheel suspension is based on a McPherson strut suspension design. The wheels are connected to an upright which has two deep-groove ball bearings supporting the wheels. The upright is attached to a damper connected to the frame, and to a ball joint attached to a leaf spring. Because the piston of the damper can freely rotate in its housing, the wheel can be steered around the centerline of the damper. The leaf spring is mounted to the frame. The pitman arm consists of two identical partial gears running against a pinion that can be actuated from within the frame. The gears and the pinions are sandwiched between two plates, to close the force loop. The pitman arm is connected to the steering arms by the steering links.

Different drivetrain concepts have been analyzed and compared. A drive train using a mechanical differential made with steel gears is most beneficial. The differential and its housing are contained in the axle. The differential is directly connected to the wheels with tubular shafts. The suspension is based on the suspension design of a truck; an A-frame is attached to the top of the axle, and two longitudinally placed struts are mounted to the bottom of the axle close to the wheels. The weight of the frame is carried by two shock absorbers.

## 7 Recommendations

An improved wheel model should be used to more accurately predict the forces that the wheels can exert on the road. Using such a model the design for the front- and rear wheel suspension can be finalized. A suggestion for such a model is the *Magic Formula* [10]. This model relies on experimental data, and therefore wheel tests should be carried out as well.

Instead of focusing on the order picking robot, different concepts should also be analyzed. The racks of the warehouse could be adapted in such a way that they can drop items one by one, instead of a worker or a robot having to pick an item from the totes. This simplifies the design of the AGV, as it only has to carry a tote to 'catch' the items falling from the racks. The AGV can thus be much lighter, and operate longer on a single charge. The picking time could even be reduced to zero by dropping an item from the rack just in time for the AGV to catch it. To still allow order pickers in the warehouse, each rack could feature buttons which trigger an item to drop. Warehouse management therefore also becomes much more efficient, as the robot and the order picker use the same mechanism.

## References

- [1] P. Brinkgreve, R. Brinkgreve, M. J. M. van der Velden: *Wegligging van Automobielen*, 1969-1972
- [2] J. L. Blanco, M. Bellone and A. Gimenez-Fernandez: *TP-Space RRT Kinematic Path Planning of Non-Holonomic Any-Shape Vehicles*, 2015
- [3] J. Ackermann, J. Guldner, W. Sienel, R. Steinhauser, and V. I. Utkin: *Linear and Nonlinear Controller Design for Robust Automatic Steering*, 1995
- [4] T. Fraichard and J. M. Ahuactzin: *Smooth Path Planning for Cars*, 2001
- [5] D. Dolgov: *Path Planning for Autonomous Vehicles in Unknown Semi-structured Environments*, 2010
- [6] G. A. den Boer, G. D. van Albada, L. O. Hertzberger, C. Koburg and M. Mergel: *The MARIE autonomous mobile robot*, 1993
- [7] I. J. M. Besselink: *Lecture notes vehicle dynamics*, 2016
- [8] J. Reimpell, H. Stoll, J. W. Betzler: *The automotive chassis: engineering principles*, 2001
- [9] C. E. Adams: *Plastic gearing: selection and application*, 1986
- [10] H. B. Pacejka: *Tyre and vehicle dynamics*, 2002

## Declaration concerning the TU/e Code of Scientific Conduct for the Master's thesis

I have read the TU/e Code of Scientific Conduct<sup>i</sup>.

I hereby declare that my Master's thesis has been carried out in accordance with the rules of the TU/e Code of Scientific Conduct

Date

18/6/2019


Name

Ties Joep van Hoon

ID-number

0861750

Signature



*Submit the signed declaration to the student administration of your department.*

<sup>i</sup> See: <http://www.tue.nl/en/university/about-the-university/integrity/scientific-integrity/>

The Netherlands Code of Conduct for Academic Practice of the VSNU can be found here also.  
More information about scientific integrity is published on the websites of TU/e and VSNU